



1     **Influence of initial soil moisture in a Regional**  
2     **Climate Model study over West Africa. Part 2:**  
3     **Impact on the climate extremes.**

4  
5     Brahima KONÉ<sup>1</sup>, Arona DIEDHIOU<sup>1, 2</sup>, Adama Diawara<sup>1</sup>, Sandrine Anquetin<sup>2</sup>, N'datchoh  
6     Evelyne Touré<sup>1</sup>, Adama Bamba<sup>1</sup> and Arsene Toka Koba<sup>1</sup>

7     <sup>1</sup>LAPAMF, Université Félix Houphouët Boigny, Abidjan, Côte d'Ivoire

8     <sup>2</sup>Univ. Grenoble Alpes, IRD, CNRS, Grenoble INP, IGE, F-38000 Grenoble, France

9     *Correspondence to:* Arona DIEDHIOU (arona.diedhiou@ird.fr)

10    **Abstract.**

11    The influence of the anomalies in initial soil moisture on the climate extreme over West Africa  
12    is investigated using the fourth generation of Regional Climate Model coupled to the version  
13    4.5 of the Community Land Model (RegCM4-CLM4.5). We applied the initial soil moisture on  
14    June 1st for two summers June-July-August-September (JJAS) 2003 and JJAS 2004 (Resp. wet  
15    and dry year in the region of interest) with 25 km of spatial resolution. We initialized the control  
16    runs with the reanalysis soil moisture of the European Centre Meteorological Weather  
17    Forecast's reanalysis of the 20th century (ERA20C), while for the dry and wet experiments, we  
18    initialized the soil moisture respectively at the wilting points and field capacity. The impact on  
19    extreme precipitation indices of the initial soil moisture, especially over the central Sahel, is  
20    homogeneous, i.e. dry (wet) experiments tend to decrease (increase) precipitation extreme  
21    indices only for precipitation indices related to the number of precipitation events, not for those  
22    related to the intensity of precipitation events. Overall, the impact on temperature extremes of  
23    the anomalies in initial soil moisture is more significant compared to precipitation extremes.  
24    Initial soil moisture anomalies unequally affect daily minimum and maximum temperature. A  
25    stronger impact is found on maximum temperature than minimum temperature. Over the entire  
26    West African domain, wet (dry) experiments cause a decrease (increase) in maximum  
27    temperature. The strongest impacts on minimum temperature indices are found mainly in wet  
28    experiments, on the Sahara where we found the higher values of the maximum and minimum  
29    daily minimum temperature indices (resp. TN<sub>x</sub> and TN<sub>n</sub>). The performance of RegCM4-  
30    CLM4.5 in simulating the ten (10) extreme rainfall and temperature indices used in this study  
31    is also highlighted.



## 32 **1 Introduction**

33 West Africa experienced large rainfall variability during the late 1960s. This variability leads  
34 often to flooding events, severe drought and regional heatwaves. Such extreme hydro-climatic  
35 events have major economic, environmental, and societal impacts (Easterling and al. 2000,  
36 Larsen 2003). In recent years, climate extremes have attracted much interest because they are  
37 expected to occur more frequently (International Panel on Climate Change (IPCC), 2012) than  
38 changes in mean climate. Yan and Yang (2000) show that for a large number of cases, the  
39 extreme climate changes were 5 to 10 times greater than climate mean change. Many key factors  
40 or physical mechanisms could be possible causes of the increase in climate extremes (Nicholson  
41 1980; Le Barbé et al. 2002), such as the effect of increasing greenhouse gases in the atmosphere  
42 on the intensification of hot extremes (IPCC, 2007), the sea surface temperature (SST)  
43 anomalies (Fontaine and Janicot 1996; Folland et al., 1986), and land surface conditions  
44 (Philippon et al. 2005; Nicholson 2000). In addition, smaller-scale physical processes, including  
45 the interactions of the coupling of land-atmosphere, can also lead to changes in climate  
46 extremes. For the European summer, the influence of soil moisture in the coupling of land-  
47 atmosphere using regional climate model and focused on the extremes and trends in  
48 precipitation and temperature have been studied by Jaeger and Seneviratne (2011). For extreme  
49 temperatures, their studies have shown that interactions of soil moisture and climate have a  
50 significant impact, while for extreme precipitation, they only influence the frequency of wet  
51 days. Over Asia, Liu and al. (2014) studied the impact on subsequent precipitation and  
52 temperature of soil moisture anomalies using a regional climate model. They show that wet  
53 (dry) experiences of anomalies in initial soil moisture decrease (increase) the hot extremes,  
54 decrease (increase) the drought extremes, and increase(decrease) the cold extremes in zone of  
55 strong soil moisture-atmosphere coupling. However, none of these papers intended to examine  
56 the impacts of the anomalies in initial soil moisture on subsequent climate extreme using a  
57 regional climate model over West Africa. In the part 1, the influence of initial soil moisture on  
58 the climate mean was based on performance assessment of the Regional Climate Model coupled  
59 with the complex Community Land Model (RegCM4-CLM4.5) done by Koné and al. (2018)  
60 where the ability of the model to reproduce the climate mean has been validated. However, in  
61 the part 2, before starting to study the influence of initial soil moisture on the climate extremes,  
62 it was needed to assess first the performance of RegCM4-CLM4.5 in simulating the ten (10)  
63 temperature indices and extreme rainfall used in this study. This has never been done before  
64 over Africa. That's why we separate in two parts, to ease the reading and to come up with papers



65 of reasonable length. The paper is organized as follows: the section 2 describes the model  
66 RegCM4, the experimental design and methodology used in this study; the section 3 presents  
67 the assessment of RegCM4-CLM4.5 in climate extremes simulation and the impacts on climate  
68 extremes of anomalies in initial soil moisture; and section 4 documents the summary and  
69 conclusions.

## 70 **2. Model, experimental design and methodology**

### 71 **2.1 Model description and numerical experiment**

72 The fourth generation of the Regional Climate Model (RegCM4) of the International Centre for  
73 Theoretical Physics (ICTP) is used in this study. Since this version, the physical representations  
74 have been subject to a continuous process of implementation and development. The release  
75 used in this study is RegCM4.7. The non-hydrostatic dynamical core of the MM5 (Mesoscale  
76 Model version 5, Grell et al., 1994) has been ported to RegCM4 while maintaining the existing  
77 hydrostatic core. We selected in this study the non-hydrostatic as model dynamical core.  
78 RegCM4 is a limited-area model using a vertical grid sigma hydrostatic pressure coordinate  
79 and a horizontal grid of Arakawa B-grid (Giorgi and al., 2012). The radiation scheme is from  
80 the NCAR-CCM3 (National Center for Atmospheric Research and the Community Climate  
81 Model Version 3) (Kiehl and al., 1996) and the aerosols representation is from Zakey and al.  
82 (2006) and Solmon and al. (2006). The large-scale precipitation scheme used in this study is  
83 from Pal and al. (2000), the moisture scheme is called the SUBgrid EXplicit moisture scheme  
84 (SUBEX) which considers the sub-grid variability in clouds, the accretion and evaporation  
85 processes for stable precipitation is from Sundqvist and al., 1989. The sensible heat and water  
86 vapor in the planetary boundary layer over land and ocean, turbulent transports of momentum  
87 are from Holtslag and al. (1990). The heat and moisture and the momentum of ocean surfaces  
88 fluxes, are from Zeng and al. (1998). Convective precipitation and the land surface processes  
89 in RegCM4.7 are represented in several options. Based on Koné and al., (2018), the convective  
90 scheme of Emanuel (Emanuel, 1991) is used. The parameterization of the land surface  
91 processes is from CLM4.5 (Oleson and al., 2013). In each grid cell of CLM4.5 there is 16  
92 different plant functional types and 10 soil layers (Lawrence et al., 2011; Wang and al., 2016).  
93 The integration of RegCM4 over the West African domain is shown in Fig. 1 with 18 vertical  
94 levels and 25 km of horizontal resolution. The European Centre for Medium-Range Weather  
95 Forecasts reanalysis (EIN75; Uppala and al., 2008; Simmons and al., 2007) provides the initial  
96 and boundary conditions. The Sea Surface Temperatures (SSTs) are derived from the National



97 Oceanic and Atmosphere Administration optimal interpolation weekly (NOAA - OI\_WK)  
98 (Reynolds and al., 1996). The topography is derived from States Geological Survey (USGS)  
99 Global Multi-resolution Terrain Elevation Data (GMTED; Danielson and al., 2011) at the  
100 spatial resolution of 30 arc-second which is an update of the Global Land Cover  
101 Characterization (GTOPO; Loveland and al., 2000) dataset.

102 The sensitivity of initial soil moisture is no longer than one season (Hong and Pan., 2000; Kim  
103 and Hong, 2006). As in part I, four months (JJAS) simulation in 2003 and 2004 have been  
104 carried out over West Africa, starting from June 1<sup>st</sup>, and the first 7 days considered as a spin-  
105 up period (Kang and al., 2014) are excluded in the analysis. Here we focused our study on  
106 climate extremes. The two years 2003 and 2004 have been chosen because they correspond  
107 respectively to a wet and dry year in the region of interest and the impact of soil moisture  
108 anomalies is investigated during the rainy season period. For each year, three experiments are  
109 carried out, we used the soil moisture from the reanalysis of the European Centre  
110 Meteorological Weather Forecast's Reanalysis of the 20<sup>th</sup> century (ERA20C) to initialize the  
111 control runs. Wet and dry experiments were initialized for the soil moisture (in volumetric  
112 fraction  $\text{m}^3 \cdot \text{m}^{-3}$ ) respectively at the field capacity ( $=0.489$ ) and the wilting point ( $=0.117 \cdot 10^{-4}$ )  
113 over the West African derived from ERA20C soil moisture dataset.

## 114 **2.2 Validation datasets and evaluation metrics**

115 Our investigation is focused on the air temperature at 2 m and the precipitation over the West  
116 African domain during the summer of JJAS for 2003 and JJAS 2004. The simulated  
117 precipitation fields are validated with two observation datasets: the Climate Hazards group  
118 Infrared Precipitation Stations (CHIRPS) dataset is from the University of California at Santa  
119 Barbara, available from 1981 to 2020 at the  $0.05^\circ$  high-resolution and the Tropical Rainfall  
120 Measuring Mission 3B43V7 (TRMM) dataset with the  $0.25^\circ$  high-resolution available from  
121 1998 to 2013 (Huffman et al., 2007). We validated the 2 m temperature with two observation  
122 datasets: the global daily temperature from the Global Telecommunication System (hereafter  
123 GTS), gridded at the horizontal resolution of  $0.5^\circ$  for 1979 to 2020 (Fan Y. and Huug van den  
124 Dool, 2008) and daily temperature from ERA-Interim (EIN) reanalysis at  $0.25^\circ$  of horizontal  
125 resolution available from 1979 to 2020 (Dee et al., 2011). For the comparison of the simulations  
126 of the model with observation datasets, we regridded all the products to  $0.22^\circ \times 0.22^\circ$ . We used  
127 an interpolation of the bilinear method for this purpose (Nikulin et al., 2012).



128 The performance of RegCM4-CLM4.5 to simulate the extreme indices has been carried using  
129 four selected sub-regions (Fig. 1) based on the previous work of Koné and al. (2018), they  
130 correspond to different features of annual cycle of precipitation. We used the mean bias (MB),  
131 which captures the small-scale differences between the simulation and the observation. The  
132 pattern correlation coefficient (PCC) is also used as a spatial correlation between model  
133 simulations and the observation to indicate the large-scale similarity degree.

134 To quantify the impact of soil moisture anomalies on climate extremes Liu and al. in their work  
135 over Asia, used the mean biases in 5 subregions, while in our study we used the mean biases  
136 and the probability density function (PDF, Gao et al. 2016; Jaeger and Seneviratne 2011) for  
137 this purpose to better capture how many grid points are impacted by initial soil moisture.

138 The two-tailed t-test is used to investigate statistically significant differences at each grid cell  
139 of the wet and dry sensitivity experiments with respect to the control one. The low result  
140 obtained (10%) must only be considered as a crude estimate. Jaeger and Seneviratne (2011)  
141 sustained that it is due to the neighboring grid points which have a spatial dependence and also  
142 to the multiplicity problem of independent tests. We can obtain a more reliable and significant  
143 estimation with methods of resampling (Wilks et al., 2006 and 1997). However, in our case it  
144 is not possible to do this because of the constraints of computation and the large size of datasets  
145 (Jaeger and Seneviratne, 2011). Therefore, we perform the land point's area-weighted fraction  
146 with statistically significance of 10% level and we display the seasonally extreme indices maps  
147 during the years 2003 and 2004.

### 148 **2.3. Extreme rainfall and temperature indices**

149 In this study, to investigate the changes in precipitation and temperature in terms of duration,  
150 occurrence and intensity, six extreme temperature and four extreme rainfall indices are  
151 examined using daily data of minimum and maximum temperature and daily rainfall (Table 1).  
152 These 10 extreme indices are recommended by the Expert Team on Climate Change Detection  
153 and Indices (ETCCDI, Peterson et al., 2001). We estimated the monthly values of the indices,  
154 which allow investigating of the seasonal variations.

155

## 156 **3. Results and discussion**

### 157 **3.1. Seasonal extreme rainfall**

158 In this section we analyze six extreme rainfall indices based on daily precipitation in RegCM4  
159 simulations over West Africa. All precipitation indices are calculated for JJAS 2003 and JJAS



160 2004. Table 2 summarizes the pattern correlation coefficient (PCC) and the mean bias (MB) of  
161 all precipitation indices studied in this section for TRMM observation and model simulations  
162 derived from control experiments with reanalysis initial soil moisture ERA20C with respect to  
163 CHIRPS observation, calculated for west Sahel, central Sahel, Guinea coast and the entire West  
164 African domain during the period JJAS 2003 and JJAS 2004.

### 165 **3.1.1 The index of the wet days occurrence (R1mm)**

166 Figure 2 shows the mean values of wet days occurrence (R1mm index, in days) from CHIRPS  
167 (Fig.2a, d) and TRMM (Fig.2b, e) observations and their corresponding simulated control  
168 experiments (Fig.2c, f) with the initial soil moisture derived from ERA20C reanalysis. The two  
169 observation datasets CHIRPS (Fig. 2a, d) and TRMM (Fig.2b, e) have a similar large-scale  
170 pattern over the West African domain with a PCC up to 0.98 (Table 2). The maximum values  
171 of wet days occurrence are located over the regions of mountains such Cameroon mountains,  
172 Jos plateau and the Guinea highlands, while the minimum values of R1mm index are found  
173 over the Sahel with the number of wet days which decrease gradually from South to North.  
174 However, although we have a similitude in their large-scale patterns, at the local scale the  
175 magnitude and extension of these maxima and minima exhibit some differences. The TRMM  
176 datasets underestimates the R1mm index values over the central and west Sahel, and  
177 overestimate them over the Guinea for both JJAS 2003 and JJAS 2004 (Table 2). For instance  
178 over the central Sahel, we observe a strong mean bias (MB) about -6.76 and 7.51 days (resp.  
179 for JJAS 2003 and JJAS 2004, Table 2), and over the Guinea coast the MB reaches 8.89 and  
180 10.44 days (resp. for JJAS 2003 and JJAS 2004, Table 2).

181 The control experiments (Fig.2c, f) reproduce well the large-scale structure of the observed  
182 rainfall with a PCCs values reaching 0.96 and 0.95 (resp. for JJAS 2003 and JJAS 2004, Table  
183 2) over the entire West African domain, but do exhibit some biases at the locale scale in term  
184 of spatial extent and magnitude. The control experiment displays a large and quite  
185 homogeneous area of maximum values of R1mm under the latitude 12°N. The control  
186 experiments overestimate the R1mm index over most of the studied domains (Table2). The  
187 largest mean biases are found over the Guinea coast with MB more than 53.16 and 55.46 days  
188 (resp. for JJAS 2003 and JJAS 2004, Table 2). This overestimation of the R1mm index in  
189 RegCM4 has been also found by Thanh and al. (2017) with RegCM4 over the Asia region.

190 Figure 2 (second panel) displays also changes in wet days occurrence for JJAS 2003 and JJAS  
191 2004, for dry (Fig.2g and i, resp. for JJAS 2003 and JJAS 2004) and wet experiments (Fig.2h  
192 and j, resp. for JJAS 2003 and JJAS 2004) compared to their control experiments associated,



193 the dotted area shows changes with statistical significance of 10% level. The dry experiments  
194 (Fig.2g, i) tend to decrease the number of wet days occurrence while the wet experiments  
195 (Fig.2h, j) tend to favor an increase of wet days occurrence, especially over the central Sahel  
196 and a small part of west Sahel. However, over the Guinea coast sub-region, both wet and dry  
197 experiments show a prevailing increase, although this increase in the dry experiments, is rather  
198 weak. Indicating that the number of wet days occurrence are occurred more likely not only in  
199 wet experiments but also in the dry experiments.

200 For a better quantitative evaluation, Figure 3 shows the PDF distributions of the changes in  
201 R1mm index over the studied domains (shown in Fig.1), during JJAS 2003 and JJAS 2004. The  
202 results essentially confirm the homogeneous impact found over the central Sahel (Fig.3a). The  
203 strongest impact on the R1mm index for the dry (wet) experiments is shown over the central  
204 (west) Sahel, with a decrease (an increase) of R1mm index and with a peak at -5 days (10 days)  
205 for the two summers JJAS 2003 and JJAS 2004. Over the West Sahel, the Guinea coast and  
206 the West African domain (resp. Fig.3b, c and d), both dry and wet experiments lead to an  
207 increase. For instance over Guinea coast a peak is shown at 3 days for both wet and dry  
208 experiments. The sensitivity of R1mm index to the contrast of year, showing by the lag between  
209 the peaks of PDFs in wet or dry experiments, is strongest over the west Sahel (Fig.3b) reaching  
210 3 days in particular in wet experiments. The wet year 2003 presents great impact as compared  
211 to dry year 2004. It is worth to note that, the differences of PDF distributions over the different  
212 domains studied highlight the importance to separate regions in sub-regions with homogeneous  
213 precipitation for analyzing.

214 Summarizing the results of this section, a strong homogeneous impact on R1mm index is found  
215 over the central Sahel, i.e. the dry experiments tend to decrease the number of wet days  
216 occurrence while the wet experiments lead to increase the wet days occurrence. This result is  
217 in line with previous work which sustained a strong coupling of land and atmosphere in areas  
218 between wet and dry climate regimes (Zhang et al., 2011; Koster and al., 2006). However, over  
219 Guinea coast, west Sahel and West African domain, both dry and wet experiments lead to cause  
220 an increase. The control experiments overestimated R1mm index over all the domain studied.

221

### 222 **3.1.2 The simple daily intensity index (SDII)**

223 We analyze in this section the SDII index which gives the amount of precipitation mean on wet  
224 days ( $R > 1\text{mm}$ ). Figure 4 (first panel) is the same as Fig.2 (first panel), but shows the amount  
225 of precipitation mean on wet days (SDII index, in mm/day). Over the entire West African



226 domain, a similar large-scale pattern is observed between the two observations products  
227 CHIRPS (Fig.4a, d) and TRMM (Fig.4b, e) with a PCC up to 0.86 for both JJAS 2003 and JJAS  
228 2004 (Table 2). However, the maxima spatial extension and the magnitude are not similar.  
229 CHIRPS (Fig.4a, d) presents large values of SDII index, reaching more than 25 mm/day in the  
230 coastline of the Gulf of Guinea, while TRMM has values not exceeding 12 mm/day over most  
231 part of this region. On the other hand, TRMM shows large sparse values of SDII index reaching  
232 up to 20 mm/day over the central and west Sahel, while CHIRPS has values not exceeding 12  
233 mm/day over this region for both JJAS 2003 and JJAS 2004. The largest biases of TRMM  
234 with respect to CHIRPS are obtained over the Guinea coast sub-region with MB more than 13  
235 and 14 mm/day (resp. for JJAS 2003 and JJAS 2004, Table2). The large-scale pattern of  
236 observation products is well reproduced by the control experiments (Fig.4 c, f) with a PCC  
237 reaching up to 0.73 and 0.77 (resp. in JJAS 2003 and JJAS 2004, Table 2) over West African  
238 domain, despite at the locale scale, they exhibit some biases. The magnitude of SDII index is  
239 quite underestimated not exceeding 10 mm/day over most of the domain studied, except over  
240 the Cameroon mountains (Fig.4c, f). As a result, precipitation events are less extreme in the  
241 control experiments. The largest mean biases are located over the Guinea coast with MB more  
242 than -13.62 and -14.65 mm/day (resp. for JJAS 2003 and JJAS 2004, Table 2).

243 Figure 4 (second panel) is the same as Fig. 2 (second panel), but displays changes in mean  
244 precipitation amount on wet days. Unlike for R1mm index, a change in the mean precipitation  
245 amount on wet days is not homogeneous over all the studied domains. In general, a similar  
246 alternation of increase and decrease of SDII index is shown for dry and wet experiments over  
247 most of the domains studied (Figure 4, second panel). It is difficult at the regional level to  
248 identify trends, however, at the local level, trends can be identified. For instance, over the  
249 Senegal and Sierra Leone, the dry (wet) experiments tend to increase (decrease) the  
250 precipitation amount on wet days (SDII index) for both JJAS 2003 and JJAS 2004.

251 As in Fig.3, Figure 5 displays PDFs of changes in SDII index. The PDFs show that a maximum  
252 of grid points over the different domains studied not presents change in precipitation amount  
253 on wet days for wet and dry experiments highlighted by the peak centered approximately on  
254 zero. The SDII index is not sensitive to contrast of the year in both wet and dry experiments  
255 over the different domains studied (Fig.5).

256 In summary, the control experiments underestimate the SDII index over all the domain study.  
257 It is worth to note that precipitation events are less extreme in the control experiments (SDII





258 index not exceeding 10 mm/day). The impact on SDII index is not homogeneous over the entire  
259 domain studied.

260

### 261 **3.1.3 The maximum duration of dry spells (CDD).**

262 The duration of dry spells (CDD index) which represents the number of consecutive days with  
263 precipitation less than 1 mm/day is analyzed in this section. Figure 6 (first panel) is the same as  
264 Fig.2 (first panel), but shows the maximum number of consecutive dry days (CDD index, in  
265 day). CHIRPS estimates show the largest values of CDD index over the Sahara more than 50  
266 days (Fig.6a, d), while the lowest values are located over the Guinea coast with CDD index less  
267 than 8 days. Over the West African domain, the two fields CHIRPS and TRMM display quite  
268 similar features over the entire West African domain with PCC more than 0.92. However, at  
269 the local scale, the two sets of observations shown some differences. In general, these  
270 differences concern the spatial extension especially over Sahel region. In JJAS 2003, the band  
271 of CDD values in the range [10; 20] days is extended too far into Sahel region for TRMM than  
272 CHIRPS. On the other hand, in JJAS 2004, TRMM (Fig.6b, e) present a narrower band of  
273 minimum CDD index values over the Guinea coast around the latitude 10°N than CHIRPS  
274 which extend this band over Guinea coast. TRMM observation underestimates the CDD index  
275 over the entire West African domain, with MB about -2.29 and -1.75 days (resp. for JJAS 2003  
276 and JJAS 2004, table2).

277 The control experiments (Fig.6c, f), over the entire West African domain, well reproduce the  
278 large-scale pattern of the observed rainfall with a PCC more than 0.85 and 0.89 (resp. for JJAS  
279 2003 and JJAS 2004, Table 1). However, in term of magnitude, some differences are shown at  
280 the locale scale. In general, the control experiments overestimate the CDD index over the whole  
281 West African domain, the central Sahel and west Sahel (Table2). While CDD index values are  
282 underestimated over the Guinea Coast (Table2). For example, the control experiments  
283 overestimate the CDD index over the West African domain with MB more than 2.63 and 7 days  
284 (resp. for JJAS 2003 and JJAS 2004, table2). The current parametrization of the model tends  
285 to increase the drought extreme over the central and west Sahel and the whole West African  
286 domain, while over the Guinea is too wet.

287 Figure 6 (second panel) is the same as Fig.2 (second panel), but shows changes in the maximum  
288 lengths of consecutive dry spells (CDD index). The initial soil moisture impact on the  
289 consecutive dry spell is homogeneous over the central and west Sahel (Fig 6, second panel), the  
290 dry (wet) experiments tends to increase (decrease) the maximum lengths of consecutive dry



291 spell (CDD index). However, over Guinea coast, the dry and wet experiments lead to a  
292 dominant decrease.

293 Figure 7 is the same as Fig.3, but displays the PDF distribution of the changes in CDD index.  
294 The impact on CDD index is homogeneous over the central and west Sahel. For instance, over  
295 the central Sahel, peaks are obtained at -6 and 2 days respectively for dry and wet experiences  
296 (Fig.7a). The weaker and non-homogeneous impact is shown over Guinea coast and the West  
297 African domain. For instance, over the Guinea coast, a decrease in CDD index values is found  
298 with a peak not exceeding 2 days for both wet and dry experiments (Fig.7c). The CDD index is  
299 sensitive to the contrast of year, especially over central Sahel and in wet experiments reaching  
300 4 days (Fig.7a). The impact in the dry year is strong than the wet year.

301 In summary, RegCM4 overestimate the CDD index over most of domain studied except over  
302 the Guinea coast. A homogeneous impact on CDD index is found over central and west Sahel,  
303 i.e. the dry (wet) experiments increase (decrease) the maximum lengths of consecutive dry spell  
304 (CDD index). However over the Guinea coast and West African Domain, we found a dominant  
305 decrease of CDD index.

306

#### 307 **3.1.4 The maximum length of wet spells (CWD).**

308 The persistence of wet spells (CWD index) which represents the number of consecutive days  
309 with precipitation  $\geq 1$  mm/day is investigated in this section. As in Fig. 2 (first panel) but for  
310 the maximum wet spell length (CWD index, in day), the spatial distribution of CWD index is  
311 shown in Figure 8 (first panel). The two observed products TRMM (Fig.8b, e) and CHIRPS  
312 (Fig.8a, d) depict a similar large-scale pattern with the PCCs reaching 0.90 and 0.87 (resp. for  
313 JJAS 2003 and JJAS 2004, Table 2). CHIRPS observation located the maximum of CWD index  
314 over the mountain regions such as Cameroon mountains, Jos plateau and Guinea highlands and  
315 it is more than 20 days, while the minimum values of CWD index are found over most of the  
316 area above the latitude 17°N and not exceed 4 days (Fig.8a, d). In general, the differences  
317 between TRMM and CHIRPS observation concern the magnitude and the maxima extent,  
318 which are more pronounced in TRMM than in CHIRPS. Generally, TRMM underestimate the  
319 CWD index than CHIRPS over most of the domains studied. The largest mean bias is found  
320 over the Guinea coast region with MB more than 2.47 and 2.38 days (resp. for JJAS 2003 and  
321 JJAS 2004, Table 2).

322 The control experiments well reproduce the large-scale pattern with PCCs values reaching up  
323 to 0.81 and 0.87 (resp. for JJAS 2003 and JJAS 2004, Table 2) over the entire West African



324 domain. However, at the local scale the control experiments exhibit some biases in term of  
325 magnitude and spatial extent of these maxima and minima. Control experiments overestimate  
326 the duration of wet days over the different domains studied. We note that this overestimation  
327 coincides with the excessive values of R1mm index (Fig.2c, f). Therefore, the overestimation  
328 of the model of R1mm index implies that CWD index which represents the maximum number  
329 of consecutive days with precipitation  $\geq 1$  mm/day can only be overestimated. The strongest  
330 mean bias is found over the Guinea coast and is more than 59.21 and 60.51 days (resp. for JJAS  
331 2003 and JJAS 2004).

332 Figure 8 (second panel) is the same as Fig.2 (second panel), but displays changes in the  
333 maximum number of consecutive wet days. As for R1mm index, over the central Sahel, the  
334 impact is homogeneous, the dry (wet) experiments tends to decrease (increase) the maximum  
335 lengths of consecutive wet spell (CWD index) for wet and dry years (resp JJAS 2003 and JJAS  
336 2004). However, over Guinea and west Sahel, the changes are not homogeneous, both dry and  
337 wet experiments lead to cause a dominant increase, in JJAS 2003 and JJAS 2004 (Fig. 8B, c).

338 Figure 9, as in Fig.3, but shows the PDF distribution of changes in CWD index. The results  
339 confirm the homogeneous impact on CWD index found over the central Sahel, the dry (wet)  
340 experiments tends to decrease (increase) the CWD index with peaks at -10 days (15 days) for  
341 both JJAS 2003 and JJAS 2004. However, over Guinea coast, west Sahel and West African  
342 domain, both dry and wet experiments tend to increase the CWD index. For instance, over the  
343 Guinea coast for wet and dry experiments peaks are respectively 12 and 2 days in JJAS 2003  
344 and JJAS 2004. The CWD index is not sensitive in contrast of year over the different domains  
345 studied.

346 Summarizing the results of this section, as in R1mm and CDD index, the CWD index is  
347 homogeneous over the central Sahel, the dry (wet) experiments tends to decrease (increase) of  
348 the CWD index. This result confirms the strong soil moisture impact over the transition zones  
349 with a climate between dry and wet regimes (Zhang et al., 2011; Koster et al., 2006). Contrary  
350 to the CDD index, over the West African Domain, west Sahel and the Guinea Coast, we found  
351 a dominant increase of CWD index. RegCM4 overestimate the duration of wet days over all  
352 the domains studied. This overestimation of CWD index is linked with an excessive number of  
353 wet days as documented by Diaconescu and al. (2014).

354

355 **3.1.5 The maximum one-day precipitation accumulation (RX1day).**



356 The maximum one-day precipitation (RX1day) during the period JJAS 2003 and JJAS 2004 is  
357 assessed in this section. Figure 10 (first panel) is identical to Figure 2 (first panel), but shows  
358 the spatial distribution of the maximum 1-day precipitation index (RX1day index, in mm). The  
359 observations datasets TRMM (Fig.10b, e) and CHIRPS (Fig.10 a, d) present a quite difference  
360 in term of the spatial extension of the maximum values of RX1day index, although their large-  
361 scale pattern is somewhat similar with PCC more than 0.84 for both JJAS 2003 and JJAS 2004  
362 (Table 2). TRMM observation extends maxima of RX1day more than 80 mm over the Guinea  
363 and the Sahel region, while CHIRPS confine them over the coastline of the Gulf of Guinea.  
364 TRMM observation overestimates the RX1day index than CHIRPS over the entire domain  
365 studied. The largest maximum one day precipitation is found over the central Sahel with MB  
366 reaching 35.78 and 31.66 (resp. for JJAS 2003 and JJAS 2004, Table 2).

367 The control experiments (Fig.10 c, f) capture the spatial pattern with PCC values 0.50 and 0.4  
368 (resp. JJAS 2003 and JJAS 2004, Table2). This low coefficient of PCC has been also obtained  
369 by Thanh and al. (2017) over Asia with RegCM4 (correlation <0.3). The models simulations  
370 failed to capture the magnitude and the spatial extent of these maxima values of RX1day index.  
371 The control experiments underestimate the RX1day index over all the domains studied. For the  
372 same reason with SDII index, the RX1day index is related to the amount of precipitation, due  
373 to the excessive light precipitation simulate by the current physical parameterization of  
374 RegCM4, the RX1day is underestimated over the entire domain studied. The largest  
375 underestimation is located over the Guinea coast and west Sahel. For instance, over the west  
376 Sahel, the MB is about -38.07 and -36.67 mm (resp. JJAS 2003 and JJAS 2004, Table 2).

377 Figure 10 (second panel) is similar to Fig. 2 (second panel), but displays changes in maximum  
378 one day precipitation. As for SDII index, the initial soil moisture anomalies impact on the  
379 RX1day index is not homogeneous, a similar mixture of increase and decrease of RX1day index  
380 is shown for dry and wet experiments over most of the domains studied (Figure 10 second  
381 panel).

382 Figure 11, as in Fig.3, but shows the PDF distribution of changes in RX1day index. As in SDII  
383 index, there is a majority of grid points which not display changes highlighted by a peak at zero  
384 (Fig.11). The RX1day index is sensitive to the contrast of years only over the west Sahel and  
385 in wet experiments. The impact on the precipitation amount on wet days in dry year (JJAS  
386 2004) is more pronounced than the wet year (JJAS 2004) reaching 5 mm (Fig.11b).



387 In summary, for the same reason with SDII index, the RX1day index is related to the amount  
388 of precipitation, the RX1day is underestimated over the entire domain studied. A non-  
389 homogeneous trend is identified over the different domains studied.

390

### 391 **3.1.6 The total precipitation due to very heavy precipitation days (R95pTOT)**

392 We now investigated in this section, the total precipitation due to very heavy precipitation days  
393 (R95pTOT index) during the period JJAS 2003 and JJAS 2004. Figure 12 (first panel) is the  
394 same as in as in Fig.2 (first panel), but shows the spatial distribution of R95pTOT index. TRMM  
395 (Fig.12b, e) and CHIRPS observations (Fig.12a, d) present a similar spatial pattern over the  
396 entire West African domain with PCC value reaching 0.91 for both JJAS 2003 and JJAS 2004  
397 (Table 2). However, there are some biases in their spatial extent. As for RX1day index, TRMM  
398 observation extends maxima of R95pTOT more than 60 mm over the Guinea and the Sahel  
399 region (Fig.10), while CHIRPS confine them over the Guinea coast. Overall, TRMM shows a  
400 dominant overestimation than CHIRPS over the West African domain about 16.54 and 18.54  
401 mm (resp. JJAS 2003 and JJAS 2004, Table2). The control experiments (Fig.12c, f) capture the  
402 spatial pattern with PCC values 0.59 and 0.55 (resp. JJAS 2003 and JJAS 2004, Table2). As  
403 with SDII and RX1day indices, the control experiments underestimate the values of the  
404 R95pTOT index, while they overestimated the R1mm index. This is also due by the current  
405 physical parameterization scheme of the RegCM4 model which results in a positive bias for the  
406 number of wet days with a low precipitation threshold (e. g. 1 mm.day<sup>-1</sup>), while for the indices  
407 of number of wet days with a higher precipitation threshold (e. g. 10 mm.day<sup>-1</sup>, not shown here),  
408 it results in a negative bias. The control experiments underestimate the R95pTOT index over  
409 the entire domain studied. The largest underestimation of R95pTOT index is located over the  
410 Guinea coast with MB more than -43 and -46 mm (resp. for JJAS 2003 and JJAS 2004, Table2).  
411 Figure 12 (second panel) is similar to Fig.2 (second panel), but displays changes in R95pTOT  
412 index. The both dry and wet experiments tend to cause an increase of R95pTOT index over the  
413 orographic regions. This means that anomalies in initial soil moisture, whether dry or wet, tend  
414 to reinforce extreme floods.

415 Figure 13, as Fig.3, but shows the PDF distribution of changes in R95pTOT index. An  
416 increasing in R95pTOT index for both wet and dry experiments is shown over most of the  
417 domains studied. The largest change is found over the west Sahel with peak reaching 5 and 2  
418 mm respectively for wet and dry experiments (Fig.13 b). The changes in R95pTOT index are  
419 sensitive to the contrast of the wet and dry year reaching 2 mm (resp. JJAS 2003 and JJAS



420 2004), especially over west Sahel (Fig. 13a). The impact on R95pTOT index in wet year is  
421 strong than dry year over the different domains studied.

422 In summary, RegCM4 underestimate the R95pTOT index over the West African domain. The  
423 anomalies in initial soil moisture, whether dry or wet, tend to reinforce extreme floods, as  
424 documented Liu and al. (2014) in their work over the Asia.

### 425 **3.2. Seasonal temperature extreme indices**

426 In this section, using daily maximum and minimum temperature, we analyze four extreme  
427 temperature indices (Table 1) in RegCM4 simulations over West Africa. All temperature  
428 indices are calculated for JJAS 2003 and JJAS 2004. The Table 3 summarizes the pattern  
429 correlation coefficient (PCC) and the mean bias (MB) of all temperature indices studied in this  
430 section for EIN reanalysis and model simulations derived from control experiments with initial  
431 soil moisture from ERA20C reanalysis, with respect to GTS observation, calculated over the  
432 domains presented in Fig 1, during the period JJAS 2003 and JJAS 2004.

433

#### 434 **3.2.1. Maximum value of daily maximum temperature (TXx index)**

435 In this section, we analyze the maximum values of daily maximum temperature (TXx index)  
436 for JJAS 2003 and JJAS 2004. Figure 14 (first panel) shows the maximum value of daily  
437 maximum temperature (TXx index in °C) from GTS observation (Fig14.a, d) and EIN  
438 reanalysis (Fig.14b, e) for JJAS 2003 and JJAS 2004 and their corresponding simulated control  
439 experiments (Fig.14c, f) with the initial soil moisture of the reanalysis ERA20C. The GTS  
440 observation shows the highest values of the TXx index observed over the Sahara at more than  
441 46° C, while the lowest values (less than 32°C) are found over the Guinea coast (Fig.14a, d).  
442 The reanalyze of EIN have similar large-scale patterns with PCC value 0.99 over the entire  
443 West African domain (Table 3). However, some biases are shown at the local scale in terms of  
444 spatial extent and magnitude of these maxima and minima. The reanalysis of the EIN (Fig.14b,  
445 e) shows lower values (less than 28°C) of the TXx index over a large area along the Guinea  
446 coastline than the GTS estimates. While GTS presents higher values of TXx index (up to 48°C)  
447 and a large surface area as compared to EIN reanalysis. The reanalysis of the EIN shows a  
448 dominant negative bias of the TXx index over most of the domains studied (Table 3).

449 The control experiments (Fig.14c, f) reasonably well replicate the large-scale models of the  
450 TXx index values with PCCs up to 0.99 over the entire West African domain, but they exhibit  
451 some bias. The control experiments are closer to the maximum and minimum values of the GTS



452 TXx index. The control simulations overestimate the TXx values over the central and west  
453 Sahel and underestimate them over the Guinea coast (Table 3). For instance, the greatest  
454 overestimation is found over the west Sahel with MB about 3.02 and 2.02°C (resp. for JJAS  
455 2003 and JJAS 2004, Table3). However, these biases obtained for TXx index in this study are  
456 much weak as compared to that found by Thanh and al. (2017) using RegCM4 over the Asia  
457 which can reach approximately 8° C.

458 Figure 14 (second panel) displays changes in TXx index for JJAS 2003 and JJAS 2004, for dry  
459 (Fig.14g, i, resp. for JJAS 2003 and JJAS 2004) and wet experiments (Fig.14h, j, resp. for JJAS  
460 2003 and JJAS 2004) with respect to their corresponding control experiments, the dotted area  
461 shows changes with statistical significance of 10% level. The impact of the anomalies in initial  
462 soil moisture on TXx index are homogeneous over the entire West African domain, i.e. the dry  
463 experiments lead to an increase of TXx index values while the wet experiments favor a decrease  
464 of TXx index values. We noted that, this homogeneous impact is more pronounced in dry and  
465 the wet experiments respectively over the Guinea coast and the central Sahel (Fig.14, second  
466 panel).

467 The PDF distributions of the changes in the maximum values of daily maximum temperature  
468 (TXx index) in JJAS 2003 and JJAS 2004, over (a) central Sahel, (b) West Sahel, (c) Guinea  
469 and (d) West Africa derived from dry and wet experiments compared to the corresponding  
470 control experiments are shown in Figure 15. As mentioned, the results confirm the  
471 homogeneous impact on TXx index of the initial soil moisture anomalies over all the domains  
472 studied. The strongest impact on TXx index of the initial soil moisture anomalies is shown over  
473 the central Sahel (Fig.15a) with a decrease (increase), with peak at -2.5°C (more than 1°C) in  
474 wet (dry) experiments. The inter-comparison of JJAS 2003 and JJAS 2004 show that change in  
475 TXx index is sensitive to the contrast of year, especially in dry experiments over the central  
476 Sahel reaching 0.8°C (Fig.15a). The impact on TXx index for the dry year (JJAS 2004) is strong  
477 than the wet year (JJAS 2003).

478 In summarizing this section, a homogeneous impact on TXx index is found over the whole  
479 West African domain, i.e. the dry (wet) experiments decrease (increase) the change in TXx  
480 index. RegCM4 overestimate and underestimate the TXx index respectively over the Sahel  
481 (west and central) and Guinea coast.

482  
483



484 **3.2.2. The Minimum value of daily maximum temperature (TXn).**

485 In this section, we analyze the minimum values of daily maximum temperature (TXn index)  
486 for JJAS 2003 and JJAS 2004. Figure 16 (first panel) is the same as in Fig.14 (first panel), but  
487 presents the spatial distribution of the TXn index. GTS observation (Fig.16a, d) and EIN  
488 reanalysis (Fig.16b, e) display similar features with PCC reaching 0.99 (for both JJAS 2003  
489 and JJAS 2004, Table 3). The maxima and minima values of TXn index are located for both  
490 respectively over the Sahara and the Guinea coast. However, some difference can be noticed at  
491 the local scale in terms of spatial extent and magnitude. EIN reanalysis presents a larger spatial  
492 extent of these maxima (greater than 36°C) and minima (less than 24°C) than GTS observation.  
493 The reanalyze of EIN show a dominant negative bias value over Guinea coast and west Sahel  
494 (for both JJAS 2003 and JJAS 2004 Table3). For instance, over the Guinea coast with MB about  
495 -0.70 and -1.38°C (resp. for JJAS 2003 and JJAS 2004, Table 3).

496 The control experiments show a good agreement with the observed (GTS) general spatial  
497 patterns with PCC about 0.99, however overestimate the magnitude of the TXn index over all  
498 the domains studied. For instance, over the whole West African domain, the MB is about 5.65  
499 and 4.14°C (resp. JJAS 2003 and JJAS 2004, Table 3). As compared to a similar study carry  
500 out by Thanh and al. (2017) over the Asia, the biases obtained in this study are weaker.

501 As in Fig.14 (second panel), but for changes in TXn index, is shown in the Figure 16 (second  
502 panel). The impact on TXn index of the initial soil moisture anomalies, as for TXx index are  
503 homogeneous over the entire West African domain, i.e. the dry experiments lead to an increase  
504 of TXn index values while the wet experiments favor a decrease of TXn index values. The  
505 strongest impact on TXn index is shown in wet experiments above the latitude 15 °N, especially  
506 for JJAS 2003.

507 Figure 17 is the same as Fig.15, but displays the PDF distribution of changes in TXn index. As  
508 for TXx index, the impact on TXn index to soil moisture anomalies is homogeneous over most  
509 of the domain studied, although this impact is rather weak as compared to the TXx index. The  
510 strongest impact on TXn index for wet experiments are found over the wet Sahel about -2°C,  
511 while in dry experiments, it is found over the central Sahel not exceed 1° C. In addition, the  
512 changes in TXn index are sensitive to the contrast of year, especially in dry experiments over  
513 west Sahel reaching 0.8°C (Fig. 13b). The impact on TXn index in dry year is strong than wet  
514 year over west Sahel.

515 In summary, RegCM4 overestimate the TXn index over the whole West African domain. As  
516 for TXx index, the impact on TXn index to soil moisture anomalies is homogeneous, i.e. the





517 dry (wet) experiments tend to cause an increase (decrease) of TXn index values over most of  
518 the domain studied. We noted that the impact on TXn index of the initial soil moisture  
519 anomalies is weak as compared with TXx index.

520

### 521 **3.2.3. The Minimum value of daily minimum temperature (TNn).**

522 In this section, we analyze the minimum values of daily maximum temperature (TNn index)  
523 for JJAS 2003 and JJAS 2004. Figure 18 (first panel) is the same as in Fig.14 (first panel), but  
524 displays the spatial distribution of the TNn index. GTS observation (Fig.18 a, d) shows the  
525 maxima of TNn index values above the latitude 15° N not exceeding 27° C, while the minima  
526 values are less than 17°C and located over the mountain regions such as Cameroon mountain,  
527 Jos Plateau and Guinea Highland. The reanalysis of EIN shows similar spatial patterns with  
528 GTS observation, with PCC value about 0.99 over the whole West African domain (Table 3)  
529 despite some biases. The reanalysis of EIN (Fig.18 b, e) displays a highest value of TNn index  
530 (exceeding 27°C) than GTS estimates and located them over large areas above the latitude 15°  
531 N. The reanalysis of EIN also shows the lowest values (less than 21°C) of TNn index than GTS  
532 observation located over the orographic regions. The reanalysis of EIN overestimates the TNn  
533 index values over most of the domain studied. For instance, over the West African domain with  
534 MB reaching 3.15 and 3.11°C (resp. for JJAS 2003 and JJAS 2004, Table 3).

535 The control experiments (Fig.18 c, f) show a good agreement with GTS observation with PCC  
536 values about 0.99, but do exhibited some biases. The control experiments overestimate the  
537 magnitude of the TNn index over all the domains studied. For instance, over the whole West  
538 African domain, the MB is about 1.45 and 0.71°C (resp. for JJAS 2003 and JJAS 2004, Table  
539 3). These dominant positive biases obtained in simulating the TXx, TXn and TNn indices are  
540 opposite with the cold bias known with RegCM4 in mean climate simulation (Koné and al.  
541 2018, Klutse and al. 2016). It is very difficult to know the origin of RCM temperature biases,  
542 as they can depend of several factors, such as surface energy fluxes and water, cloudiness,  
543 surface albedo (Sylla et al. 2012; Tadross et al. 2006).

544 Figure 18 (second panel) is the same as in Fig.14 (second panel), but displays changes in TNn  
545 index. The impact on TNn index of anomalies in initial soil moisture is homogeneous over the  
546 Sahara region, i.e. the wet experiments lead to an increase of TNn index values while the dry  
547 experiments favor a decrease of TNn index values. We noticed this homogeneous impact  
548 coincides with the area of highest TNn index values. However, over the central and west Sahel,



549 both dry and wet experiments lead to a dominant decrease. Conversely, over the Guinea coast,  
550 we found a dominant increase.

551 Figure 19 is the same as Fig.15, but shows the PDF distribution of changes in TNn index. The  
552 impact on changes in TNn index, are not homogeneous over all the domains studied. However,  
553 although this impact is weak, over central and west Sahel it tends to decrease, while over the  
554 Guinea coast it tends to increase. For instance, the strongest impact is found over the west Sahel,  
555 where the wet and dry leads to a decrease in TNn index, with peaks at  $-1^{\circ}\text{C}$  and  $-0.2^{\circ}\text{C}$   
556 respectively.

557 In summary, RegCM4 overestimate the TNn index over the entire domain studied. The impact  
558 on TNn index to the soil moisture anomalies is homogeneous only over the Sahara, i.e. the dry  
559 (wet) experiments tend to decrease (increase) the TNn index values. We noticed, this  
560 homogeneous impact coincides with the area of highest TNn index values. However, over the  
561 central and west Sahel, both dry and wet experiments lead to a dominant decrease, while over  
562 the Guinea coast, they lead to a dominant increase.

563

#### 564 **3.2.4. The Maximum value of daily minimum temperature (TNx)**

565 In this section, we turn our attention on the maximum values of daily maximum temperature  
566 (TNx index) for JJAS 2003 and JJAS 2004. Figure 20 (first panel) is the same as in Fig.14  
567 (first panel), but for TNx index. GTS observation (Fig.20 a, d) shows the maxima of TNx index  
568 values over the Sahara reaching up  $40^{\circ}\text{C}$ , while the minima values reaching  $24^{\circ}\text{C}$  are located  
569 over the Guinea coast sub-region. The reanalysis of EIN (Fig.20 b, e) shows a similar large  
570 scale patterns with PCC value reaching 0.99, but some biases can be noticed between GTS and  
571 EIN datasets. The reanalysis of the EIN underestimates the maxima (not exceeding  $38^{\circ}\text{C}$ ) and  
572 the minima (less than  $22^{\circ}\text{C}$ ) located respectively over the Sahara and the orographic regions  
573 such as Cameroon mountains, Jos plateau and Guinea highlands. The strongest negative mean  
574 bias is located over the Guinea coast with MB about  $-3.11$  and  $-3.14^{\circ}\text{C}$  (resp. JJAS 2003 and  
575 JJAS 2004, Table 3).

576 As with previous temperature indices, the control experiments (Fig.20 c, f) well reproduce the  
577 general features of TNx index with a PCC value reaching 0.99, but do exhibited some  
578 differences at the local scale. In contrast to the TNN index, the control experiments  
579 underestimate the TNx index, over most of the domains studied. The maxima of TNx index  
580 values are quite underestimate over the Sahara. For instance, over the central Sahel, the MB is



581 about  $-3.85$  and  $-3.99^{\circ}\text{C}$  (resp. for JJAS 2003 and JJAS 2004, Table 3). This underestimation  
582 of TNx seems to be systematic related to the cold bias in RegCM4 over West Africa which is  
583 shown by several papers (Koné and al. 2018, Klutse and al. 2016).

584 Figure 20 (second panel) is the same as Fig.14, but displays changes in TNx index, as in Fig.14  
585 (second panel). As for TNn index, the impact on TNx index of anomalies in initial soil moisture  
586 is somewhat homogeneous over the Sahara, i.e. the dry experiments lead to an increase of TNx  
587 index values while the wet experiments favor a decrease of TNx index values. However over  
588 the central and west Sahel, both wet and dry experiments lead to a dominant decrease, although  
589 in the dry experiment, the signal is rather weak. Conversely, over the Guinea coast, the impact  
590 on TNx index tends to cause a dominant increase.

591 Figure 21 is the same as Fig.15, but displays the PDF distributions of the changes in TNx index.  
592 As with TNn index, the impact on TNx index changes, is not homogeneous over the entire  
593 domains studied. We noticed that TNX index is more sensitive to the wet and dry experiments  
594 over the central Sahel than the other sub-regions studied. The strongest impact in the wet  
595 experiments, is found over the central Sahel (Fig. 21 a) and it's about  $-1.3^{\circ}\text{C}$ , while in dry  
596 experiments it's found over the west Sahel more than  $-1^{\circ}\text{C}$  (Fig. 21 b).

597 In summary, RegCM4 underestimates the TNx index values over the entire domain studied. As  
598 for TNn index, the impact on TNx index to the soil moisture anomalies is homogeneous only  
599 over the Sahara, i.e. the dry (wet) experiments tend to decrease (increase) the TNn index values.  
600 However, over the central and west Sahel, both dry and wet experiments lead to a decrease,  
601 while over the Guinea coast, this impact tends to cause a dominant increase. As compared to  
602 TNn index, the impact on TNx index of the anomalies in initial soil moisture is stronger.

603 Overall, anomalies in initial soil moisture unequally affect the daily maximum and minimum  
604 temperature over the West African domain. A strong impact is found on daily maximum  
605 temperature extremes than the daily minimum temperature extremes. These results are in line  
606 with the previous works (Jaeger and Seneviratne, 2011; Zhang et al., 2009).

#### 607 **4. Summary and conclusions**

608 The impact on the subsequent summer extreme climate of the anomalies in initial soil moisture  
609 over West Africa is investigated using the RegCM4-CLM45. In addition, the performance of  
610 RegCM4-CLM4.5 in representing six extreme indices of precipitation and four extreme indices  
611 of temperature over West Africa was also evaluated. Results have been presented for the two  
612 summers, JJAS 2003 (wet year) and JJAS 2004 (dry year). We performed a sensitivity studies



613 over the West African domain, with 25 km of spatial resolution. We initialized the control runs  
614 by ERA20C reanalysis soil moisture, and at its wilting points and the field capacity respectively  
615 for dry and wet experiments.

616 Compared to the extreme indices of the observation datasets, the model overestimated and  
617 underestimated the number of wet days occurrence with respectively a low ( $1\text{mm}\cdot\text{day}^{-1}$ ) and  
618 high threshold rain rate (e.g.  $10\text{ mm/day}$ , not shown here). RegCM4 also underestimated the  
619 simple precipitation intensity index (SDII), the maximum 1-day precipitation (Rx1day) and the  
620 total precipitation due to very heavy precipitation days (R95pTOT). The current physical  
621 parameterization scheme of the RegCM4 model results in a positive bias for the number of wet  
622 days with a low precipitation threshold (e. g.  $1\text{ mm}\cdot\text{day}^{-1}$ ), while for the indices of number of  
623 wet days with a higher precipitation threshold (e. g.  $10\text{ mm}\cdot\text{day}^{-1}$ , not shown here), it results in  
624 a negative bias. However, the CWD and CDD indices were generally overestimated over the  
625 whole West African domain. On the other hand, the model RegCM4 overestimated the  
626 temperature extreme indices used in this study (TXx, TXn and TNn), except for TNx index,  
627 which is underestimated over the West African domain. As a result, temperature events are  
628 more extreme in the control experiments, except in TNx index.

629 The impact on extreme precipitation indices of anomalies in initial soil moisture, especially  
630 over the central Sahel, are homogeneous, i.e. dry (wet) experiments tend to decrease (increase)  
631 precipitation extreme indices only for precipitation indices related to the number of  
632 precipitation events (R1mm, CDD and CWD indices), not for those related to the intensity of  
633 precipitation events (SDII, RX1day and R95pTOT indices). Therefore, these results confirm  
634 the strong coupling of land and atmosphere in areas between wet and dry climate regimes (e.g.  
635 Zhang et al., 2011; Koster et al., 2006). In the west Sahel sub-region, the impact of soil moisture  
636 anomalies is homogeneous only for the CDD index, i.e. dry (wet) experiments lead to an  
637 increase (decrease) in the CDD index. While dry and wet experiments result in an increase in  
638 the R1mm, CWD and R95pTOT indices. In the Guinea coast, dry and wet experiments tend to  
639 cause an increase in CWD, R1mm and R95pTOT, except for the CDD index, where they cause  
640 a decrease. We noted that the impact on extreme precipitation indices of anomalies in initial  
641 soil moisture is homogeneous only for indices related to the number of precipitation events  
642 (R1mm, CDD and CWD indices), and not for those related to the amount of precipitation per  
643 event (SDII, RX1day and R95pTOT). It is also important to note that dry and wet experiments



644 amplify very heavy precipitation days (R95pTOT index) over most of the domain studied. In  
645 addition, among all the precipitation indices studied, the year's contrast has a significant impact  
646 only for the CDD index on the central Sahel for wet experiments.

647 The impact on extreme temperatures of anomalies in initial soil moisture is generally greater  
648 than on extreme precipitation. Initial soil moisture anomalies unequally affect daily minimum  
649 and maximum temperature. A strong impact is found on maximum temperature than minimum  
650 temperature. Wet (dry) experiments result in an increase (decrease) in the TXx and TXn indices  
651 in most of the areas studied. Contrary to the indices related to the maximum temperature (TXx  
652 and TXn), the impact of soil moisture on the indices related to the minimum temperature (the  
653 TNx and TNn indices) is not homogeneous over most of the domains studied. The strongest  
654 impacts on minimum temperature indices are found over the Sahara where the TNn and TNx  
655 indices values are higher and their changes are somewhat homogeneous. In fact, initial moisture  
656 anomalies in dry (wet) soils tend to cause an increase (a decrease) in the TNn and TNx indices  
657 over the Sahara. However, in west and central Sahel, both dry and wet experiments tend to  
658 decrease the TNn and TNx indices, but increase them over the Guinea coast.

659 Overall, the impact on precipitation of the anomalies in initial soil moisture is much more  
660 complicated, as compared to temperature. For a proper assessment of the dependence of the  
661 model in our results, it would be appropriate to repeat the investigation using different RCMs  
662 in a multi-model framework.

#### 663 **Author contribution**

664 The authors declare to have no conflict of interest with this work. B. Koné and A. Diedhiou  
665 fixed the analysis framework. B. Koné carried out all the simulations and figures production  
666 according to the outline proposed by A. Diedhiou. B. Koné and A. Diedhiou, S. Anquetin and  
667 A. Diawara worked on the analyses. All authors contributed to the drafting of this manuscript.

#### 668 **Acknowledgements**

669 The research leading to this publication is co-funded by the NERC/DFID “Future Climate for  
670 Africa” programme under the AMMA-2050 project, grant number NE/M019969/1 and by  
671 IRD (Institut de Recherche pour le Développement; France) grant number UMR IGE  
672 Imputation 252RA5.

673



674 **References:**

675 Danielson J.J., and Gesch D.B.: Global multi-resolution terrain elevation data 2010  
676 (GMTED2010): U.S. Geological Survey Open-File Report 2011–1073, 26 p, 2011.

677

678 Dee D. P., Uppala S. M., Simmons A. J., Berrisford P., Poli P., Kobayashi S., Andrae U.,  
679 Balmaseda, M. A., Balsamo G., Bauer, P., Bechtold P., Beljaars A. C. M., van de Berg L.,  
680 Bidlot J., Bormann N., Delsol C., Dragani R., Fuentes M., Geer A. J., Haimberger L., Healy S.  
681 B., Hersbach H., Hólm E. V., Isaksen L., Kållberg P., Köhler M., Matricardi M., McNally A.  
682 P., Monge-Sanz B. M., Morcrette J.-J., Park, B.-K., Peubey C., de Rosnay P., Tavolat C.,  
683 Thépaut J.-N. and Vitart F.: The ERA-Interim reanalysis: configuration and performance of the  
684 data assimilation system, Q. J. Roy. Meteorol. Soc., 137, 553-597,  
685 <https://doi.org/10.1002/qj.828>, 2011.

686

687 Diaconescu E. P., Gachon P. , Scinocca J., and LapriseR.: Evaluation of daily precipitation  
688 statistics and monsoon onset/retreat over western Sahel in multiple data sets. *Climate Dyn.*, 45,  
689 1325–1354, doi:10.1007/s00382-014-2383-2, 2015 .

690

691 Easterling, D.R., Meehl, G.A., Parmesan, C., Changnon, S.A., Karl, T.R. and Mearns, L.O.:  
692 Climate Extremes: Observations, Modeling and Impacts. *Science* , 289, 2068-2074.  
693 <https://doi.org/10.1126/science.289.5487.2068>, 2000.

694

695 Emanuel K. A.: A scheme for representing cumulus convection in large-scale models. *Journal*  
696 *of the Atmospheric Science* 48: 2313–2335, 1991.

697

698 Fan Y., and van den Dool H. : A global monthly land surface air temperature analysis for 1948  
699 -present, *J. Geophys. Res.* 113, D01103, doi: 10.1029/2007JD008470, 2008.

700

701 Folland C. K., Palmer T. N. , and Parker D. E.: Sahel rainfall and worldwide sea  
702 temperatures, *Nature*, 320, 602 – 607, 1986.

703

704 Fontaine B., Janicot S. , and Moron V. : Rainfall anomaly patterns and wind field signals over  
705 West Africa in August (1958 – 1989), *J. Clim.*, 8, 1503 –1510, 1995.

706



- 707 Giorgi F., Coppola E., Solmon F., Mariotti L., Sylla M. B., Bi X., Elguindi N., Diro G. T., Nair  
708 V., Giuliani G., Cozzini S., Guettler I., O'Brien T., Tawfik A., Shalaby A., Zakey A. S., Steiner  
709 A., Stordal F., Sloan L., and Brankovic C. : RegCM4: model description and preliminary tests  
710 over multiple CORDEX domains, *Clim. Res.*, 52, 7–29, doi.org/10.3354/cr01018, 2012.  
711
- 712 Grell G., Dudhia J. and Stauffer D. R.: A description of the fifth generation Penn State/NCAR  
713 Mesoscale Model (MM5), National Center for Atmospheric Research Tech Note NCAR/TN-  
714 398+STR, NCAR, Boulder, CO, 1994.  
715
- 716 Holtslag A., De Bruijn E., and Pan H. L. : A high resolution air mass transformation model for  
717 short-range weather forecasting, *Mon. Weather Rev.*, 118, 1561–1575, 1990.  
718
- 719 Hong S. Y. and Pan H. L.: Impact of soil moisture anomalies on seasonal, summertime  
720 circulation over North America in a regional climate model. *J. Geophys. Res.*, 105 (D24), 29  
721 625–29 634, 2000.  
722
- 723 Huffman, G. J., Adler, R. F., Bolvin, D. T., Gu, G., Nelkin, E. J., Bowman, K. P., Hong, Y,  
724 Stocker, E. F., and Wolff, D. B.: The TRMM multisatellite precipitation analysis: quasi-  
725 global, multiyear, combined-sensor precipitation estimates at fine scale, *J. Hydrometeorol.*, 8,  
726 38–55, 2007.  
727
- 728 Jaeger E. B., and Seneviratne S. I. : Impact of soil moisture-atmosphere coupling on  
729 European climate extremes and trends in a regional climate model, *Clim. Dyn.*, 36(9-10),  
730 1919-1939, doi:10.1007/s00382-010-0780-8, 2011.  
731
- 732 Kang S, Im E.-S. and Ahn J.-B.: The impact of two land-surface schemes on the characteristics  
733 of summer precipitation over East Asia from the RegCM4 simulations *Int. J. Climatol.* 34:  
734 3986–3997, 2014.  
735
- 736 Koné B., Diedhiou A., N'datchoh E. T., Sylla M. B. , Giorgi F., Anquetin S., Bamba A.,  
737 Diawara A., and Koba A. T.: Sensitivity study of the regional climate model RegCM4 to  
738 different convective schemes over West Africa. *Earth Syst. Dynam.*, 9, 1261–1278.  
739 <https://doi.org/10.5194/esd-9-1261-2018>, 2018.



740

741 Kiehl J. T., Hack J. J., Bonan G. B., Boville, B. A., Briegleb B. P., Williamson D. L., and Rasch  
742 P. J.: Description of the NCAR Community Climate Model (CCM3), Technical Note  
743 NCAR/TN-420+STR, 152, 1996.

744

745 Koster R. D., GUO Z. H., Dirmeyer P. A., Bonan G., Chan E., Cox P., Davies H., Gordon C.  
746 T., Gordon C. T., Lawrence D., Liu P., Lu C. H., Malyshev S., McAvaney B., Mitchell K, Mocko  
747 D., Oki K., Oleson K., Pitman A., Sud Y. C. , Taylor C. M., 16 Versegby D., Vasic R., Xue  
748 Y., Yamada T.: The global land-atmosphere coupling experiment. Part I: Overview, J.  
749 Hydrometeorol., 7(4), 590–610, doi:10.1175/JHM510.1, 2006.

750

751 Larsen J.: Record heat wave in Europe takes 35,000 lives. Earth Policy Institute, 2003.

752

753 Le Barbé L., Lebel L., and Tapsoba D.: Rainfall variability in west africa during the years 1950-  
754 1990. J. Climate, 15 :187–202., 2002.

755

756 Loveland TR, Reed BC, Brown JF, Ohlen DO, Zhu Z, Yang L, J. W. Merchant J. W.:  
757 Development of a global land cover characteristics database and IGBP DISCover from 1km  
758 AVHRR data. International Journal of Remote Sensing 21: 1303–1330, 2000.

759

760 Liu D., G. Wang R. Mei Z. Yu, and Yu M. : Impact of initial soil moisture anomalies on climate  
761 mean and extremes over Asia, J. Geophys. Res. Atmos., 119, 529–545,  
762 doi:10.1002/2013JD020890, 2014.

763

764 Klutse B. A. N., Sylla B. M., Diallo I., Sarr A., Dosio A., Diedhiou A., Kamga A., Lamptey B.,  
765 Ali A., Gbobaniyi E. O., Owusu K., Lennard C., Hewitson B., Nikulin G., & Panitz H.-J.,  
766 Büchner M.: Daily characteristics of West African summer monsoon precipitation in CORDEX  
767 simulations. Theor Appl Climatol. 123:369–386 DOI 10.1007/s00704-014-1352-3, 2016.

768

769 Nicholson, SE.: The nature of rainfall fluctuations in subtropical West-Africa. Mon. Wea. Rev.  
770 22109, 2191-2208, 1980.

771





- 772 Nicholson S.E.: Land Surface processes and Sahel climate. *Reviews of Geophysics*. 38(1), 117-  
773 24139, 2000.
- 774
- 775 Nikulin G., Jones C., Samuelsson P., Giorgi F., Asrar G., Büchner M., Cerezo-Mota R.,  
776 Christensen O. B., Déque M., Fernandez J., Hansler A., van Meijgaard E., Sylla M. B. and  
777 Sushama L.: Precipitation climatology in an ensemble of CORDEX-Africa regional climate  
778 simulations, *J. Climate*, 6057–6078, <https://doi.org/10.1175/JCLI-D-11-00375.1>, 2012.
- 779
- 780 Oleson K., Lawrence D. M., Bonan G. B., Drewniak B., Huang M., Koven C. D., Yang Z.-L.:  
781 Technical description of version 4.5 of the Community Land Model (CLM) (No. NCAR/TN-  
782 503+STR). doi:10.5065/D6RR1W7M, 2013.
- 783
- 784 Pal J. S., Small E. E. and Elthair E. A.: Simulation of regional scale water and energy budgets:  
785 representation of subgrid cloud and precipitation processes within RegCM, *J. Geophys. Res.*,  
786 105, 29579–29594, 2000.
- 787
- 788 Peterson T. C., Folland C., Gruza G., Hogg W. Mokssit A., Plummer N. : Report on the  
789 activities of the working group on climate change detection and related rapporteurs 1998-2001.  
790 Geneva (Switzerland): WMO Rep. WCDMP 47, WMO-TD 1071, 2001.
- 791
- 792 Philippon N., Mougou E. , Jarlan L. , and Frison P.-L.: Analysis of the linkages between  
793 rainfall and land surface conditions in the West African monsoon through CMAP, ERS-  
794 WSC, and NOAA-AVHR R data. *J. Geophys. Res.*, 110, D24115,  
795 doi:10.1029/2005JD006394, 2005.
- 796
- 797 Reynolds, R. W. and Smith, T. M.: Improved global sea surface temperature analysis using  
798 optimum interpolation, *J. Climate*, 7, 929–948, 1994.
- 799
- 800 Simmons A. S., Uppala D. D. and Kobayashi S.: ERA-interim: new ECMWF reanalysis  
801 products from 1989 onwards, *ECMWF Newsl.*, 110, 29–35, 2007.



- 802 Solmon F., Giorgi F., and Liousse C.: Aerosol modeling for regional climate studies:  
803 application to anthropogenic particles and evaluation over a European/African domain, *Tellus*  
804 *B*, 58, 51–72, 2006.
- 805
- 806 Sundqvist H. E., Berge E., and Kristjansson J. E.: The effects of domain choice on summer  
807 precipitation simulation and sensitivity in a regional climate model, *J. Climate*, 11, 2698–2712,  
808 1989.
- 809
- 810 Sylla MB, Giorgi F, Stordal F.: Large-scale origins of rainfall and temperature bias in high  
811 resolution simulations over Southern Africa. *Climate Res.* 52: 193–211, DOI: 10.3354/cr01044,  
812 2012.
- 813
- 814 Tadross MA, Gutowski WJ Jr, Hewitson BC, Jack C, New M.: MM5 simulations of interannual  
815 change and the diurnal cycle of southern African regional climate. *Theor. Appl. Climatol.* 86(1–  
816 4):63–80, 2006.
- 817
- 818 Thanh N.-D., Fredolin T. T., Jerasorn S., Faye C., Long T.-T., Thanh N.-X., Tan P.-V., Liew  
819 J., Gemma N., Patama S., Dodo G. and Edwin A.: Performance evaluation of RegCM4 in  
820 simulating extreme rainfall and temperature indices over the CORDEX-Southeast Asia region.  
821 *Int. J. Climatol.* 37: 1634–1647. Published online 28 June 2016 in Wiley Online Library  
822 (wileyonlinelibrary.com) DOI: 10.1002/joc.4803, 2017.
- 823
- 824 Uppala S., Dee D., Kobayashi S., Berrisford P. and Simmons A.: Towards a climate data  
825 assimilation system: status update of ERA-interim, *ECMWF Newsl.*, 15, 12–18, 2008.
- 826
- 827 Wang, G., Yu, M., Pal, J. S., Mei, R., Bonan, G. B., Levis, S., and Thornton, P. E.: On the  
828 development of a coupled regional climate vegetation model RCM-CLM-CN-DV and its  
829 validation its tropical Africa, *Clim. Dynam.*, 46, 515–539, 2016.
- 830
- 831 Wilks DS. : *Statistical Methods in the Atmospheric Sciences (Second Edition)*, Academic  
832 Press, 627p, 2011.
- 833



834 Yan Z., and C. Yang, Geographic patterns of climate extreme changes in China during 1951–  
835 1997, *Clim. Environ. Res.*, 5(3), 267–272, 2000.

836

837 You Q., Kang S., Aguilar E., Pepin N., Flügel W.-A., Yan Y. , Xu Y., Zhang Y. , and Huang  
838 J. : Changes in daily climate extremes in China and their connection to the large scale  
839 atmospheric circulation during 1961–2003, *Clim. Dyn.*, 36(11-12), 2399–2417,  
840 doi:10.1007/s00382-009-0735-0, 2010.

841

842 Zakey A. S., Solmon F., and Giorgi F.: Implementation and testing of a desert dust module in  
843 a regional climate model, *Atmos. Chem. Phys.*, 6, 4687–4704, [https://doi.org/10.5194/acp-6-](https://doi.org/10.5194/acp-6-4687-2006)  
844 4687-2006, 2006.

845

846 Zeng X., Zhao M. and Dickinson R .E.: Intercomparison of bulk aerodynamic algorithms for  
847 the computation of sea surface fluxes using TOGA COARE and TAO DATA, *J. Climate*, 11,  
848 2628-2644, 1998.

849

850 Zhang J, Wang W.C., and Wu L.: Land–atmosphere coupling and diurnal temperature range  
851 over the contiguous United States. *Geophys Res Lett* 36:L06706. doi:10.1029/2009GL037505,  
852 2009.

853

854 Zhang J. Y., Wu L. Y. and Dong W. : Land-atmosphere coupling and summer climate  
855 variability over East Asia, *J. Geophys. Res.*, 116,D05117, doi 10.1029/2010JD014714, 2011.

856

857

858

859

860

861

862

863



864 **TABLES AND FIGURES.**  
 865

Extreme indices	Definition	Units
Extreme Rainfall Indices		
1 R1mm	count of days when daily precipitation $\geq 1$ mm	day
2 SDII	total precipitation divided by total number of rain days with daily precipitation above 1mm	mm/day
3 CDD	maximum length of dry spell, maximum number of consecutive days with $R < 1$ mm day <sup>-1</sup>	day
4 CWD	maximum length of wet spell, maximum number of consecutive days with $R \geq 1$ mm day <sup>-1</sup>	day
5 RX1day	Maximum 1 day precipitation amount	mm
6 R95pTOT	Total precipitation due to days with precipitation exceeding the 95th percentiles for wet-day amounts.	mm
Extreme temperature indices		
7 TXn	Minimum value of daily maximum temperature	°C
8 TXx	Maximum value of daily maximum temperature	°C
9 TNn	Minimum value of daily minimum temperature	°C
10 TNx	Maximum value of daily minimum temperature	°C

866

867 **Table1:** The 10 extreme climate indices used in this study.

868

869



870

871

		Central Sahel		West Sahel		guinea		West Africa	
		MB	PCC	MB	PCC	MB	PCC	MB	PCC
R1mm	TRMM_2003	-6.76	0.98	-3.15	0.99	8.89	0.99	-1.12	0.98
	CTRL_2003	33.17	0.98	-5.25	0.96	53.16	0.96	22.18	0.96
	TRMM_2004	-7.51	0.98	-3.42	0.99	10.44	0.98	-1.34	0.98
	CTRL_2004	29.50	0.98	1.34	0.96	55.46	0.96	23.85	0.95
SDII	TRMM_2003	2.67	0.96	0.22	0.94	-5.24	0.95	1.20	0.86
	CTRL_2003	-7.52	0.97	-9.95	0.94	-13.62	0.77	-7.67	0.73
	TRMM_2004	2.07	0.96	0.45	0.96	-6.44	0.94	1.16	0.86
	CTRL_2004	-7.01	0.97	-9.37	0.94	-14.65	0.81	-7.59	0.77
CDD	TRMM_2003	1.21	0.95	0.89	0.93	-0.93	0.94	-2.29	0.92
	CTRL_2003	0.93	0.90	14.49	0.91	-7.84	0.66	2.63	0.85
	TRMM_2004	2	0.95	1.58	0.96	-3.17	0.92	-1.75	0.94
	CTRL_2004	4.75	0.91	17.51	0.95	-9.43	0.68	6.99	0.89
CWD	TRMM_2003	-0.48	0.92	0.80	0.94	2.47	0.92	0.37	0.90
	CTRL_2003	45.56	0.83	18.44	0.75	59.21	0.88	31.20	0.81
	TRMM_2004	-0.68	0.92	0.97	0.92	2.38	0.89	0.26	0.87
	CTRL_2004	36.78	0.79	20.48	0.78	60.51	0.82	29.74	0.79
RX1day	TRMM_2003	35.78	0.92	25.31	0.89	14.31	0.86	26.02	0.84
	CTRL_2003	-26.46	0.78	-38.07	0.91	-30.28	0.54	-20.08	0.50
	TRMM_2004	31.66	0.91	20.19	0.91	10	0.88	22.19	0.85
	CTRL_2004	-22.89	0.46	-36.67	0.88	-42.44	0.42	-20.23	0.40
R95pTOT	TRMM_2003	23.19	0.92	13.31	0.94	-0.23	0.96	16.54	0.91
	CTRL_2003	-27.67	0.67	-33.39	0.77	-43.22	0.65	-29.12	0.59
	TRMM_2004	23.26	0.91	12.32	0.94	-0.93	0.95	18.54	0.91
	CTRL_2004	-24.38	0.46	-31.75	0.80	-46.61	0.60	-27.45	0.55

872

873 **Table 2:** The pattern correlation coefficient (PCC) and the mean bias (MB) of R1mm (in day),  
 874 SDII (in mm/day), CDD (in day), CWD (in day), RX1day (in mm) and R95pTOT (in mm)  
 875 indices for TRMM observation and their corresponding control experiments (initialized with  
 876 initial soil moisture of ERA20C reanalysis) with respect to CHIRPS, calculated over Guinea  
 877 coast, central Sahel, west Sahel and the entire West African domain for JJAS 2003 and JJAS  
 878 2004.



879

880

		Central Sahel		West Sahel		guinea		West Africa	
		MB	PCC	MB	PCC	MB	PCC	MB	PCC
TXx	TRMM_2003	-2.17	0.99	-3.05	0.99	-4	0.99	-2.77	0.99
	CTRL_2003	2.10	0.99	3.02	0.99	-1.34	0.99	0.32	0.99
	TRMM_2004	-2.44	0.99	-3.86	0.99	-3.84	0.99	-2.94	0.99
	CTRL_2004	1.14	0.99	2.02	0.99	-1.41	0.99	-0.16	0.99
TXn	TRMM_2003	0.31	0.99	-1.48	0.99	-0.70	0.99	0.50	0.99
	CTRL_2003	5.12	0.99	6.56	0.99	3.76	0.99	5.65	0.99
	TRMM_2004	-0.76	0.99	-1.73	0.99	-1.38	0.99	-0.32	0.99
	CTRL_2004	3.43	0.99	5.44	0.99	2.75	0.99	4.14	0.99
TNn	TRMM_2003	3.08	0.99	3.43	0.99	1.28	0.99	3.15	0.99
	CTRL_2003	2.37	0.99	3.30	0.99	1.53	0.99	1.45	0.99
	TRMM_2004	3.28	0.99	2.98	0.99	1.20	0.99	3.11	0.99
	CTRL_2004	2.09	0.99	2.55	0.99	1.28	0.99	0.71	0.99
TNx	TRMM_2003	-0.69	0.99	-1.79	0.99	-3.11	0.99	-1.62	0.99
	CTRL_2003	-1.91	0.99	-2.86	0.99	-3.35	0.99	-3.85	0.99
	TRMM_2004	-0.82	0.99	-1.43	0.99	-3.14	0.99	-1.71	0.99
	CTRL_2004	-1.90	0.99	-2.54	0.99	-3.32	0.99	-3.99	0.99

881

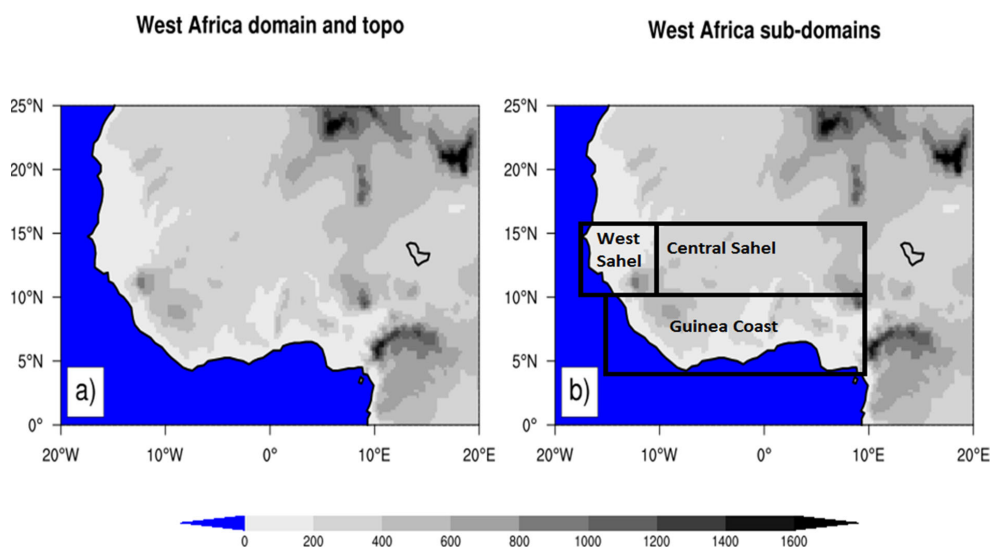
882 **Table 3:** The pattern correlation coefficient (PCC) and the mean bias (MB in °C) of TXx,  
 883 TXn, TNn and TNx indices from the reanalyze of EIN and their corresponding control  
 884 experiments (initialized with initial soil moisture of ERA20C reanalysis) with respect to GTS,  
 885 calculated for Guinea coast, central Sahel, west Sahel and the entire West African domain for  
 886 JJAS 2003 and JJAS 2004.

887



888

889



890

891

892 **Figure 1:** Topography of the West African domain. The analysis of the model result has an  
893 emphasis on the whole West African domain and the three subregions Guinea coast, central  
894 Sahel and west Sahel, which are marked with black boxes.

895

896

897

898

899

900

901

902

903

904

905

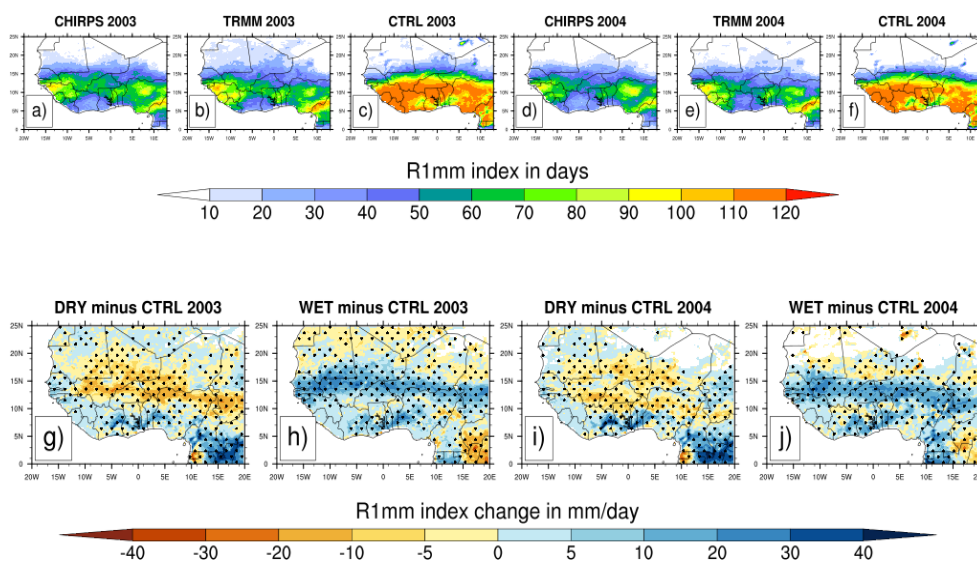
906

907

908



909  
910  
911



912  
913

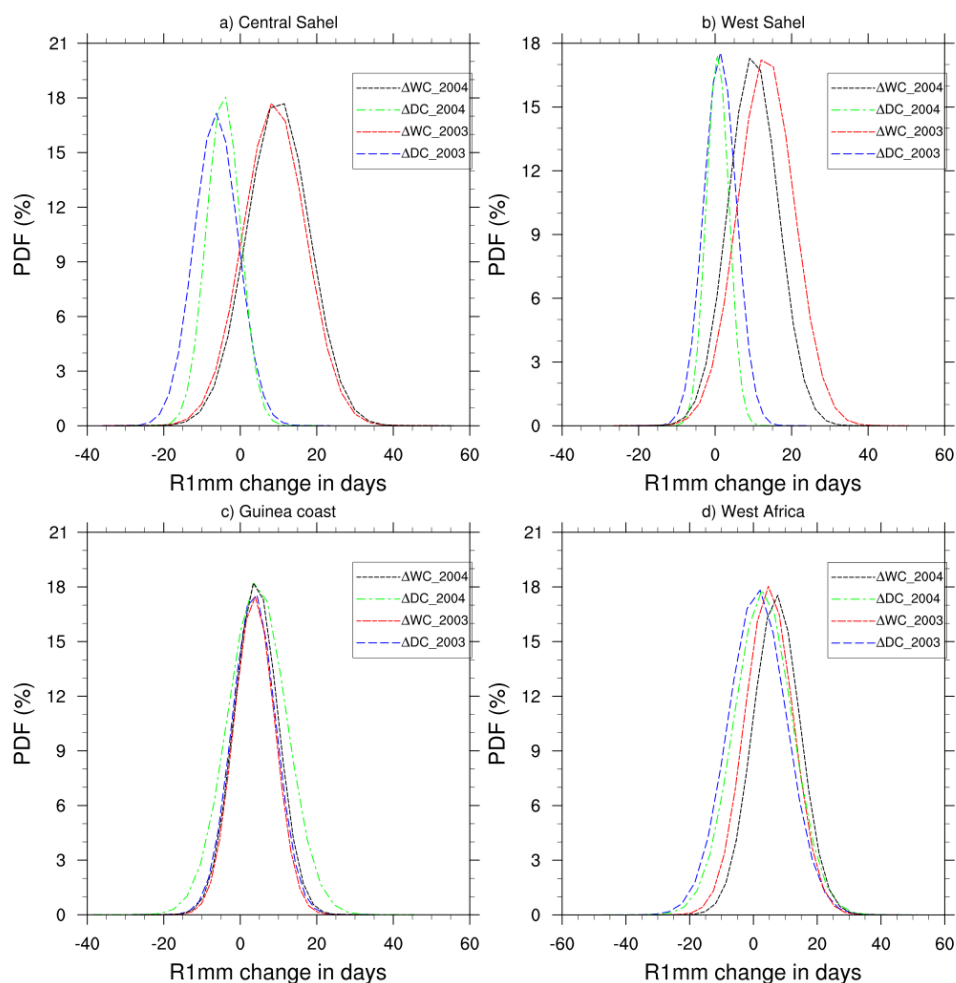
914 **Figure2:** Observed 4-month averaged (JJAS) mean values of wet days occurrence (R1mm  
915 index in days) from CHIRPS (a and d) and TRMM(b and e) observations for JJAS 2003 and  
916 JJAS 2004 and their corresponding simulated control (CTRL) experiments (c and f) initialized  
917 with initial soil moisture of the reanalysis of ERA20C (first panel) and changes in R1mm index  
918 in days (second panel) for JJAS 2003 and JJAS 2004, from dry (g and i) and wet (h and j)  
919 experiments with respect to the corresponding control experiments. Areas with values passing  
920 the 10% significance test are dotted.

921  
922  
923  
924  
925  
926  
927  
928  
929





930  
931  
932

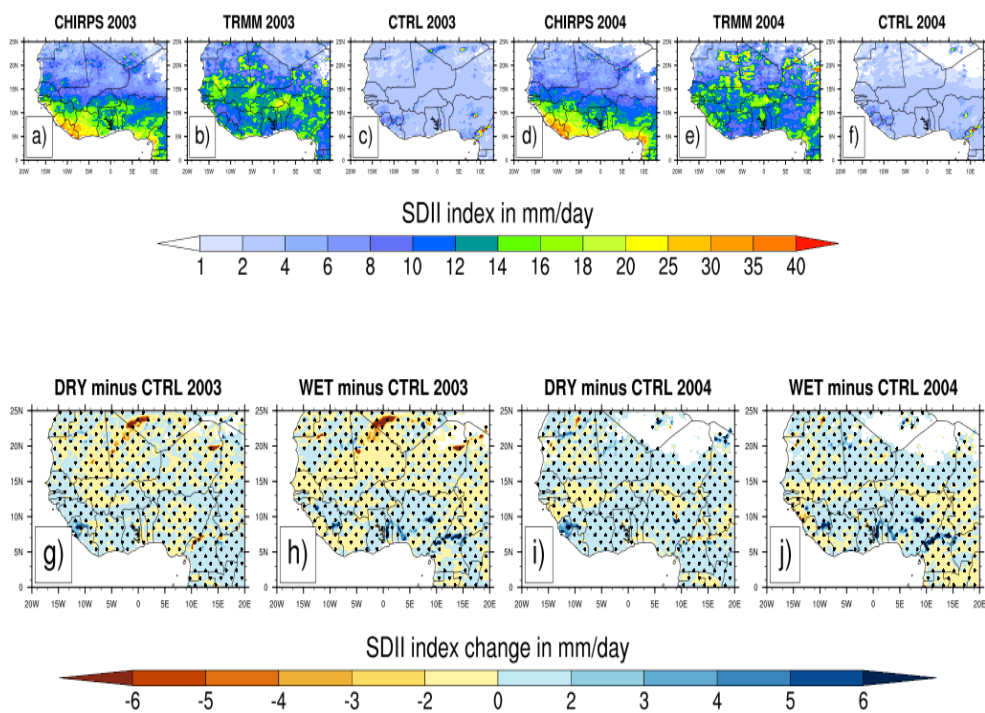


933  
934  
935  
936  
937  
938  
939  
940

**Figure3:** PDF distributions (%) of mean values of wet days occurrence change in JJAS 2003 and JJAS 2004, over (a) central Sahel, (b) West Sahel, (c) Guinea and (d) West Africa derived from dry ( $\Delta DC$ ) and wet ( $\Delta WC$ ) experiments with respect to their corresponding control experiment.



941  
942  
943

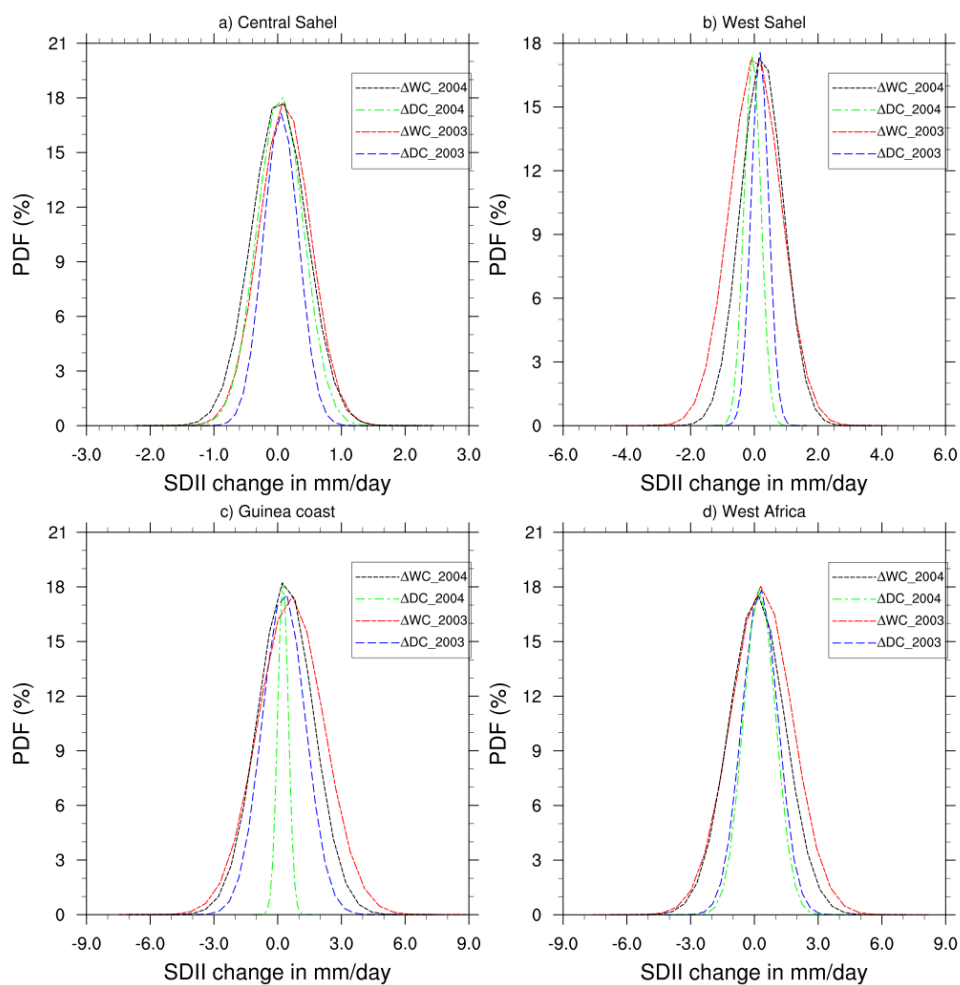


944  
945  
946  
947  
948  
949  
950  
951  
952  
953  
954  
955  
956  
957  
958

**Figure4:** Same as Fig. 2 but for the SDII index (in mm/day).



959  
960  
961

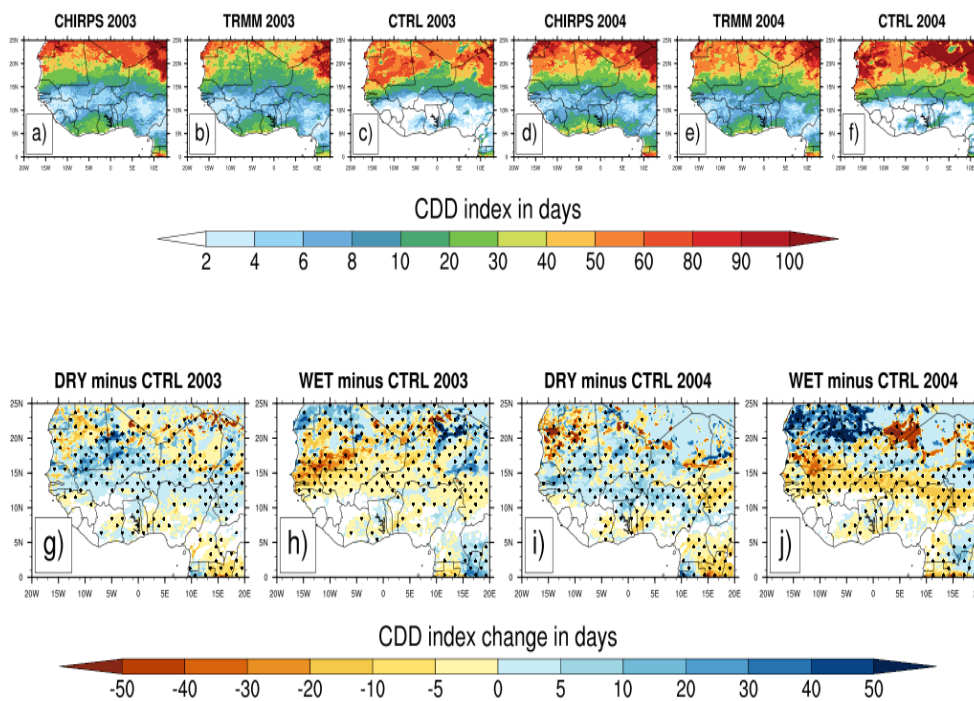


962  
963  
964  
965  
966  
967  
968  
969  
970

**Figure 5:** Same as Fig. 3 but for the SDII index (in mm/day).



971  
972  
973

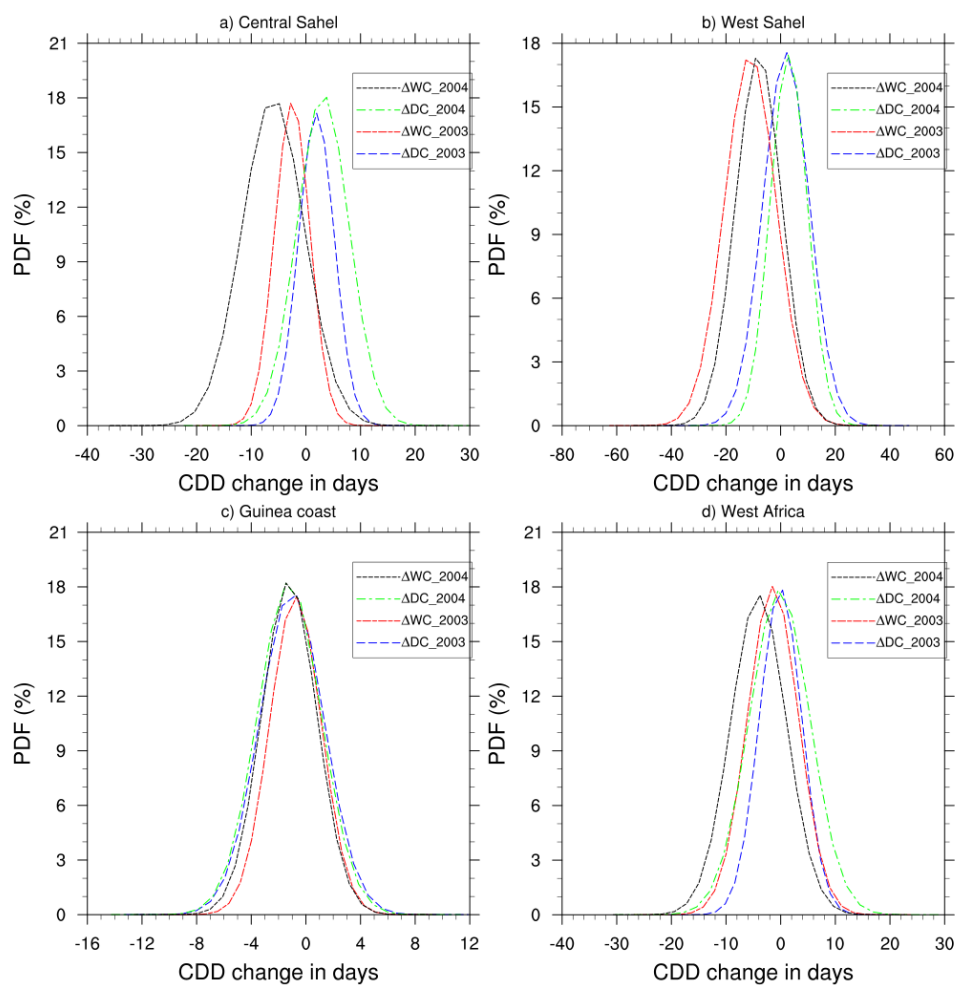


974  
975  
976  
977  
978  
979  
980  
981  
982  
983  
984  
985  
986  
987  
988

**Figure 6:** Same as Fig. 2 but for the CDD index (in day).



989  
990  
991

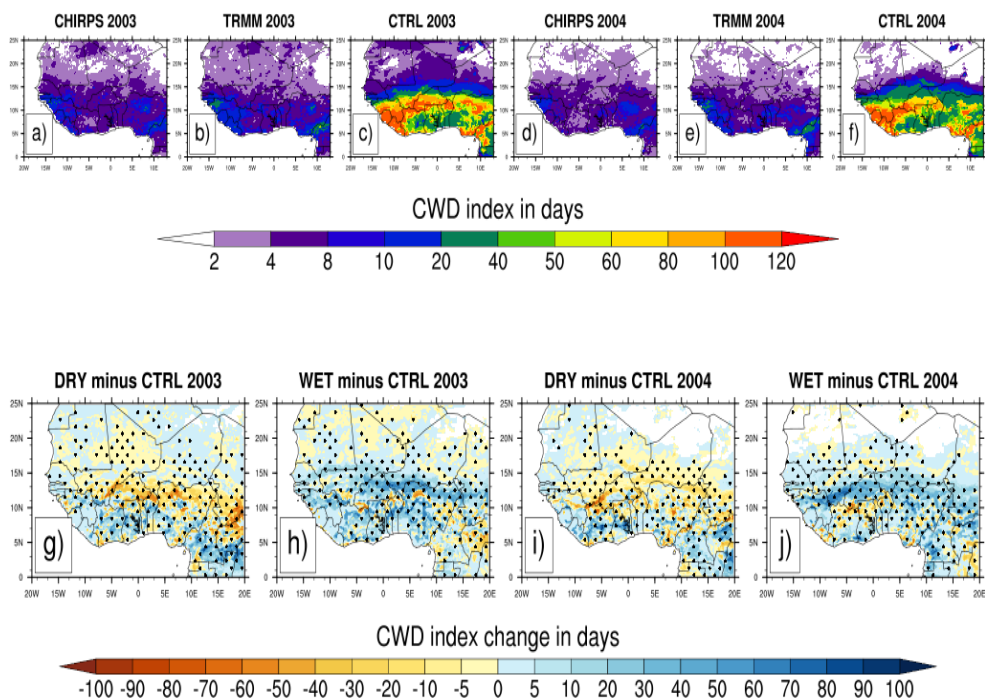


992  
993  
994  
995  
996  
997  
998  
999

**Figure 7:** Same as Fig. 3 but for the CDD index (in day).



1000  
1001  
1002

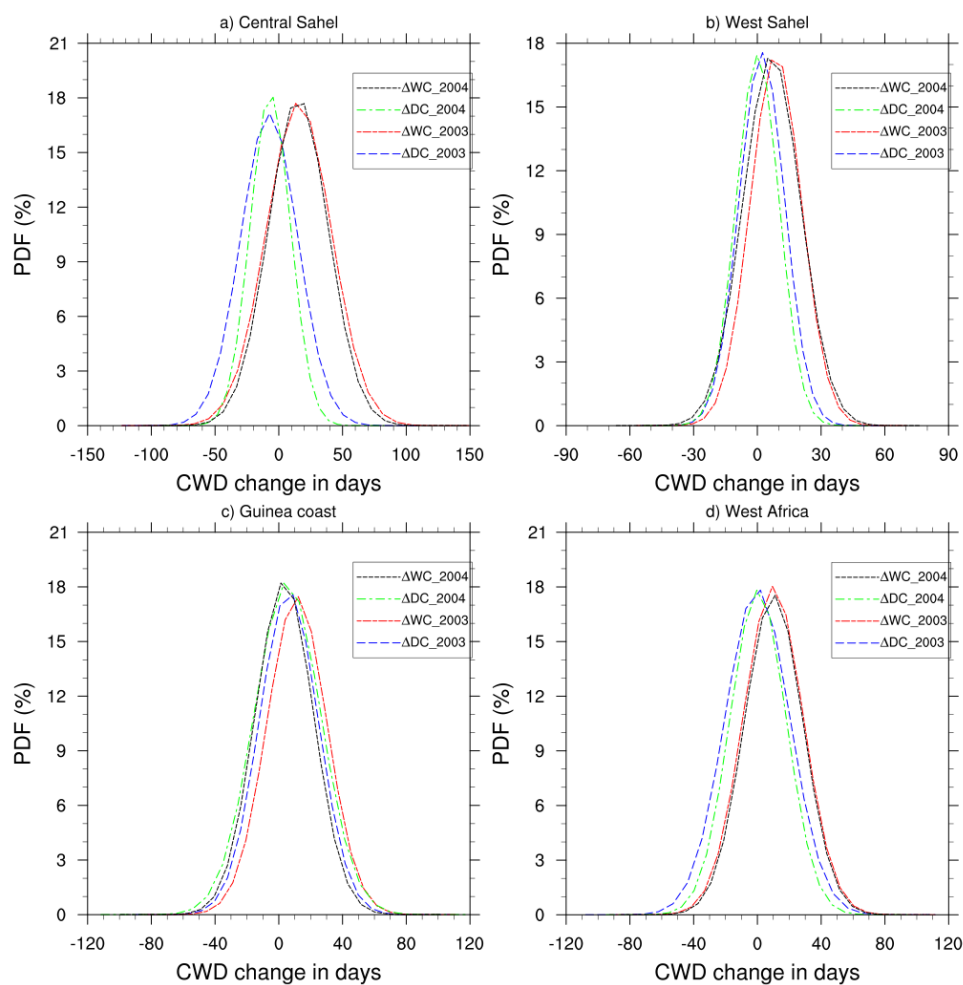


1003  
1004  
1005  
1006  
1007  
1008  
1009  
1010  
1011  
1012  
1013  
1014  
1015  
1016  
1017  
1018

**Figure 8:** Same as Fig. 2 but for the CWD index (in day).



1019  
1020  
1021

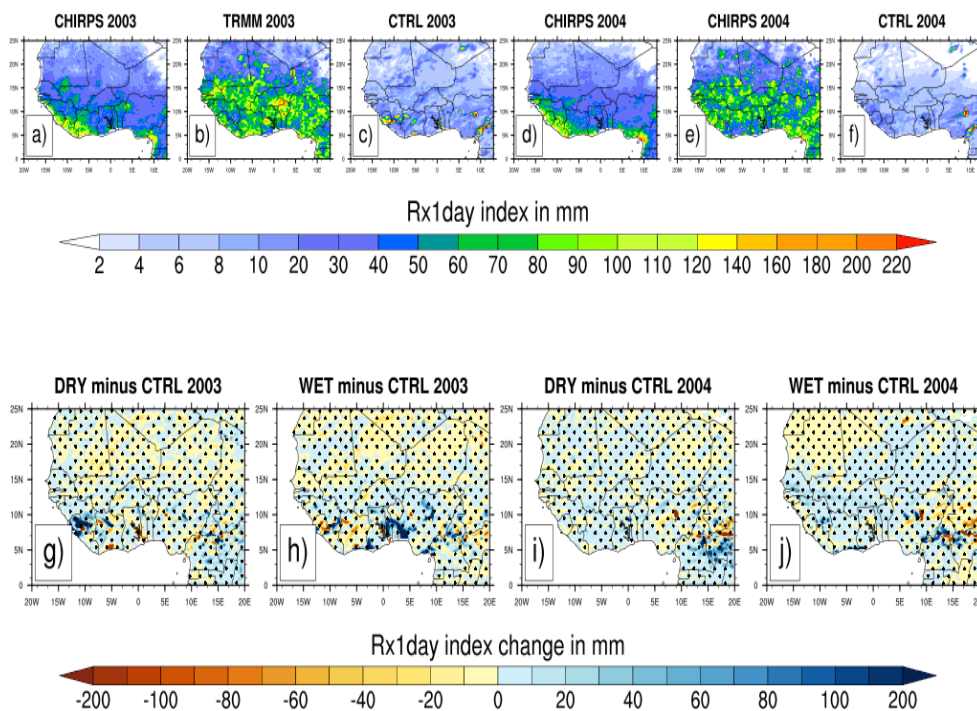


1022  
1023  
1024  
1025  
1026  
1027  
1028  
1029  
1030

**Figure 9:** Same as Fig. 3 but for the CWD index (in day).



1031  
1032  
1033



1034  
1035  
1036  
1037  
1038  
1039  
1040  
1041  
1042  
1043  
1044  
1045  
1046  
1047

**Figure 10:** Same as Fig. 2 but for the RX1day index (in mm).

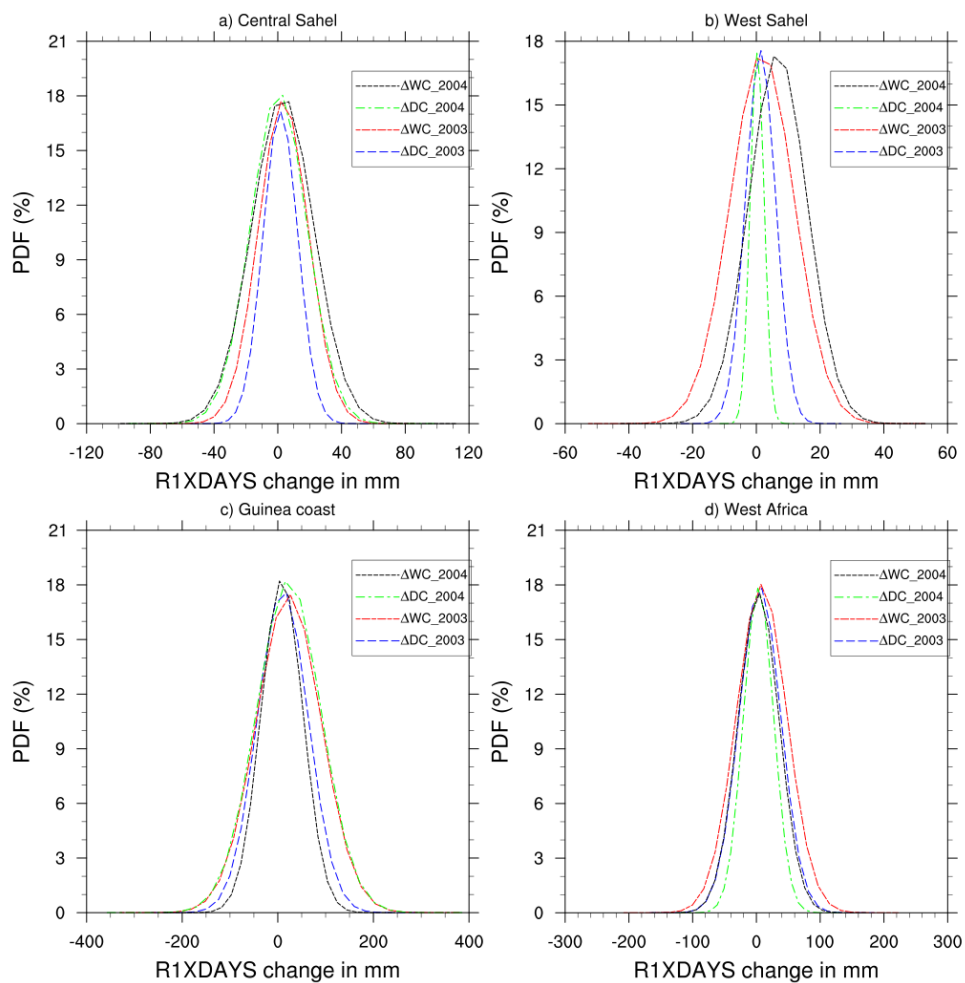




1048

1049

1050



1051

1052

1053 **Figure 11:** Same as Fig. 3 but for the RX1DAY index (in mm).

1054

1055

1056

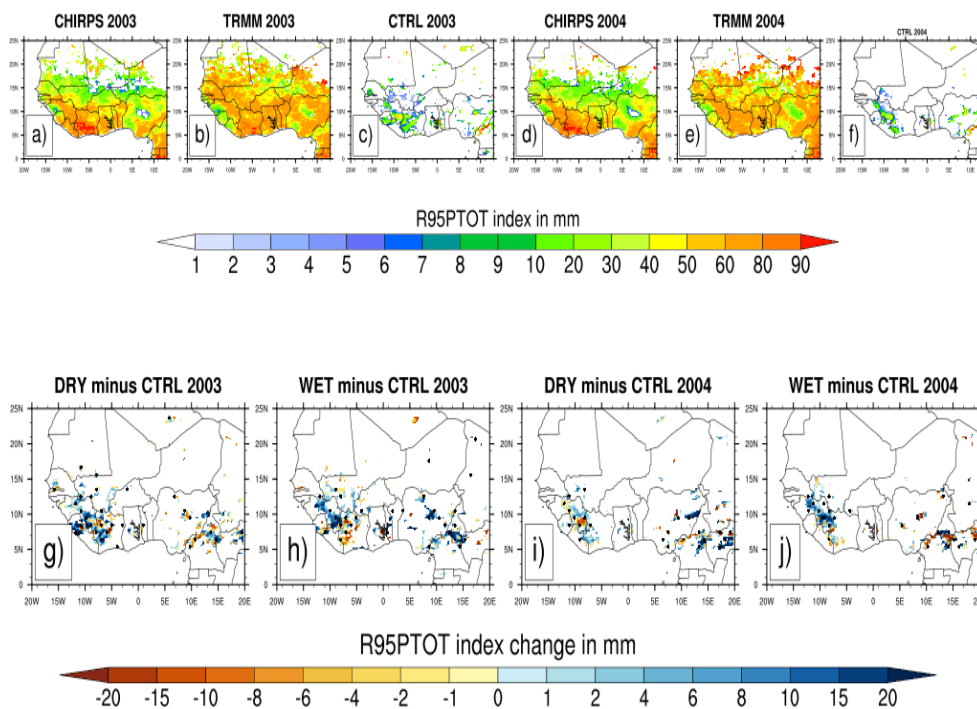
1057

1058

1059



1060  
1061  
1062

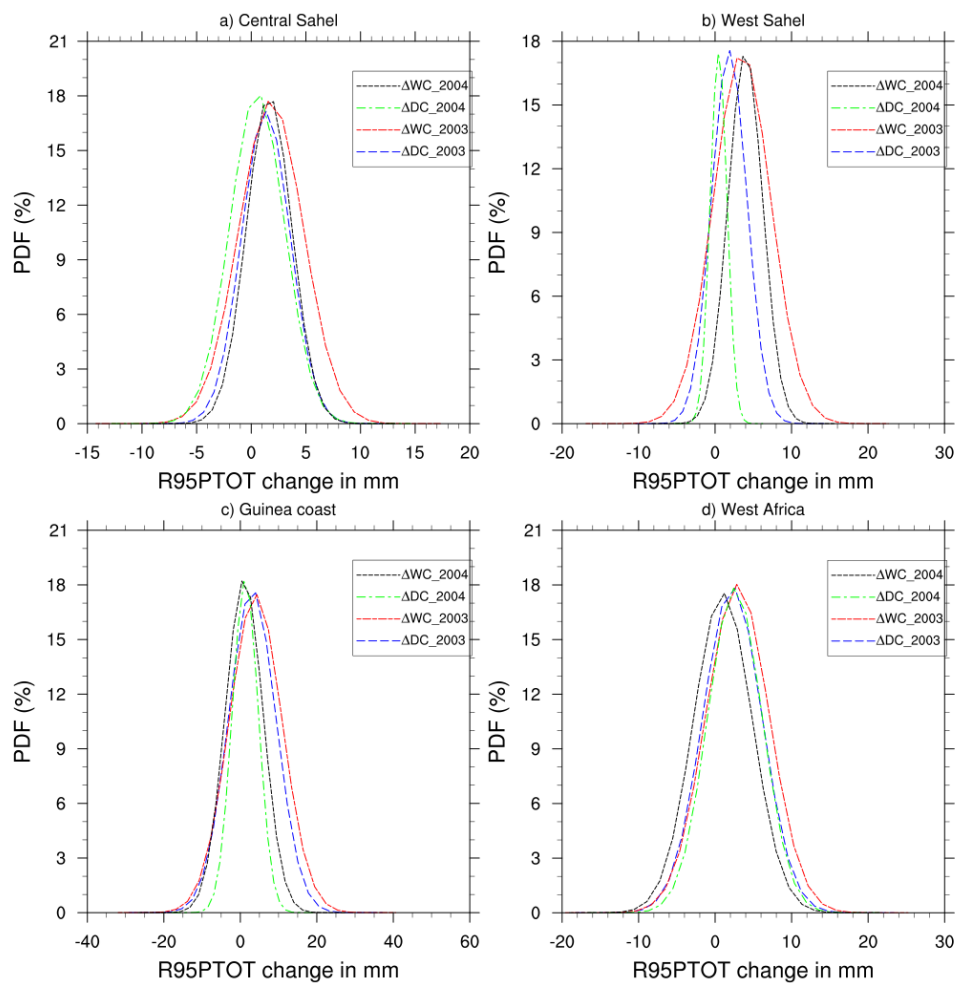


1063  
1064  
1065  
1066  
1067  
1068  
1069  
1070  
1071  
1072  
1073  
1074  
1075  
1076  
1077  
1078

**Figure 12:** Same as Fig. 2 but for the R95pTOT index (in mm).



1079  
1080  
1081

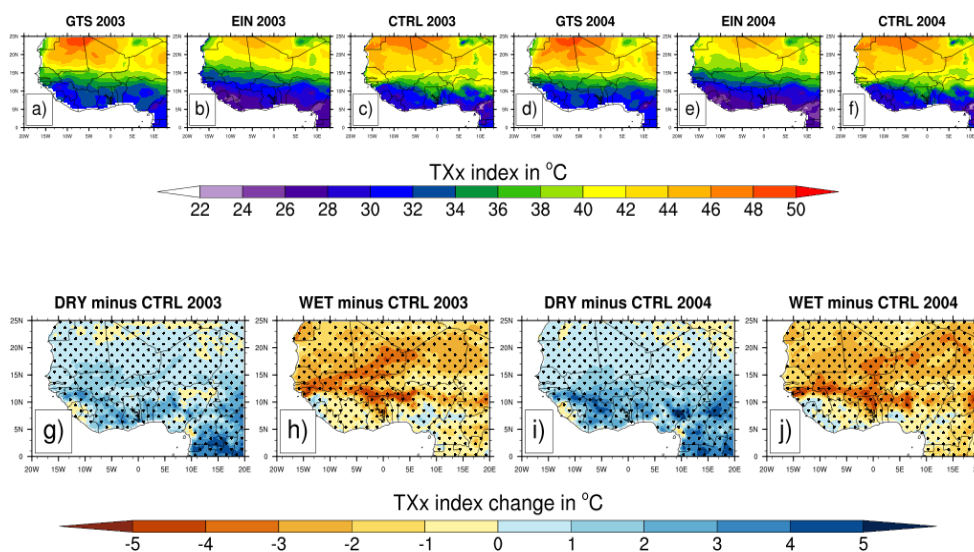


1082  
1083  
1084  
1085  
1086  
1087  
1088  
1089

**Figure 13:** Same as Fig. 3 but for the R95pTOT index (in mm).



1090  
1091  
1092

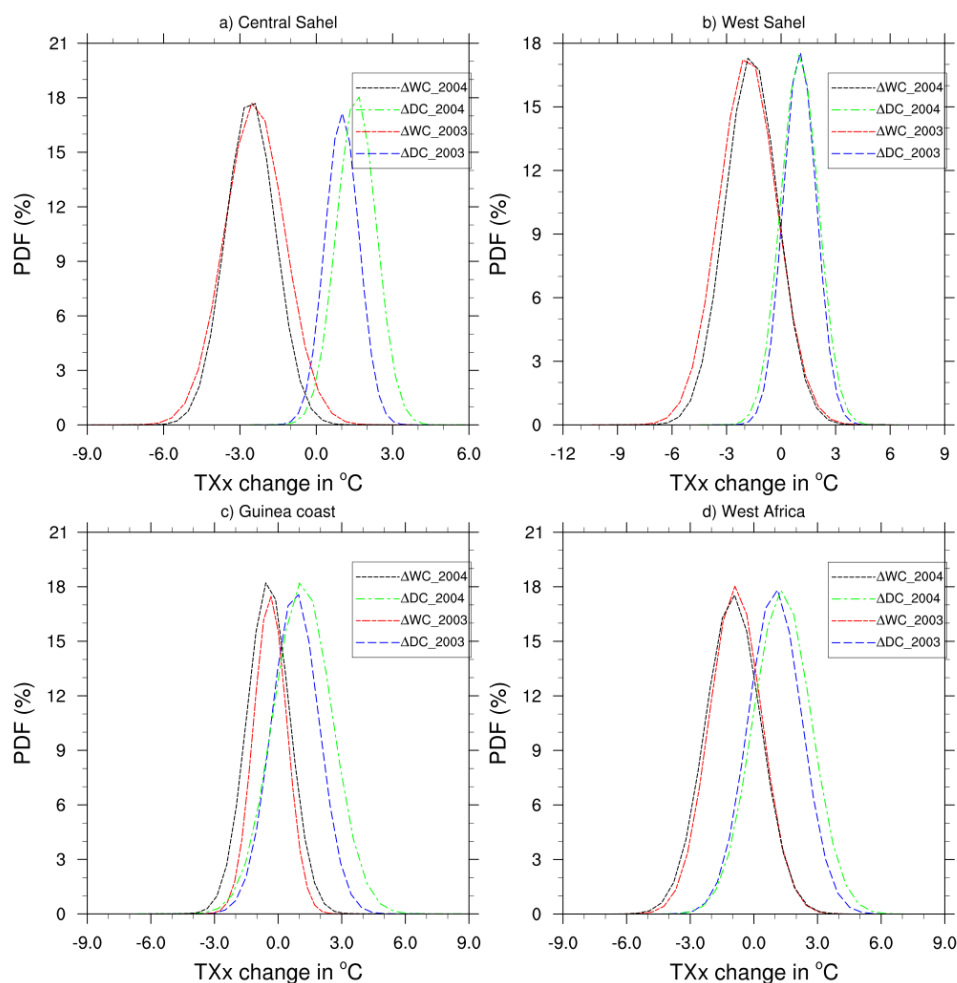


1093  
1094  
1095  
1096  
1097  
1098  
1099  
1100  
1101  
1102  
1103  
1104  
1105  
1106  
1107  
1108  
1109  
1110  
1111

**Figure 14:** Observed 4-month averaged (JJAS) maximum value of daily maximum temperature (TXx index in °C) from GTS observation (a and d) and the reanalysis of EIN (b and e) for JJAS 2003 and JJAS 2004 and their corresponding simulated control (CTRL) experiments (c and f) initialized with the initial soil moisture of the ERA20C reanalysis (first panel) and changes in TXx index in °C (second panel) for JJAS 2003 and JJAS 2004, from dry (g and i) and wet (h and j) experiments with respect to the corresponding control experiments. Areas with values passing the 10% significance test are dotted.



1112  
1113  
1114



1115  
1116  
1117  
1118  
1119  
1120  
1121  
1122

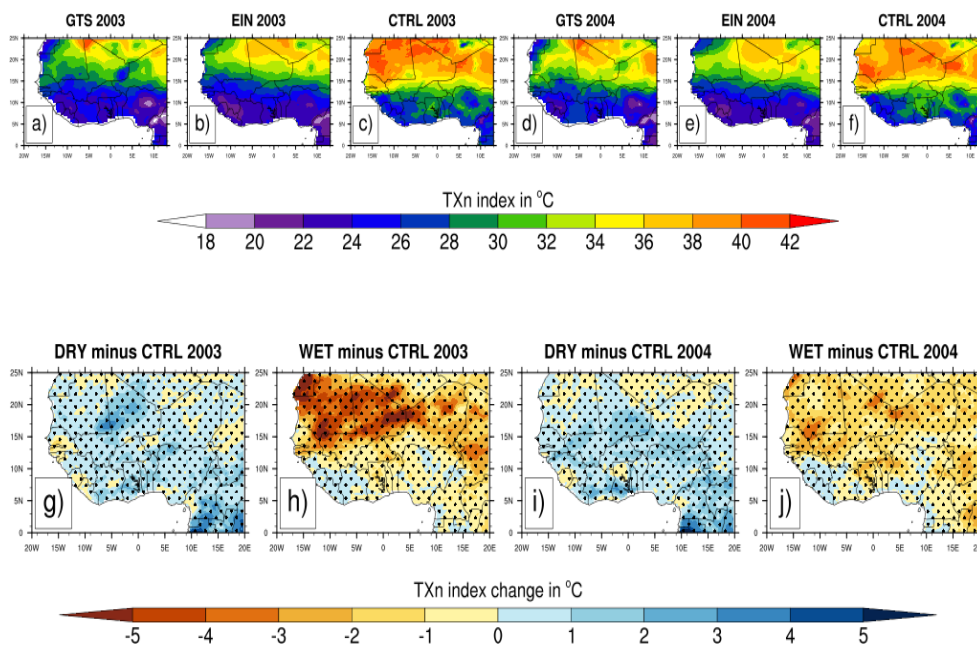
**Figure 15:** PDF distributions (%) of change in maximum value of daily maximum temperature (TXx index, in °C) for JJAS 2003 and JJAS 2004, over (a) central Sahel, (b) West Sahel, (c) Guinea and (d) West Africa derived from dry (ΔDC) and wet (ΔWC) experiments compared to their corresponding control experiment.



1123

1124

1125



1126

1127

1128

1129 **Figure 16:** Same as Fig. 14 but for the TXn index

1130

1131

1132

1133

1134

1135

1136

1137

1138

1139

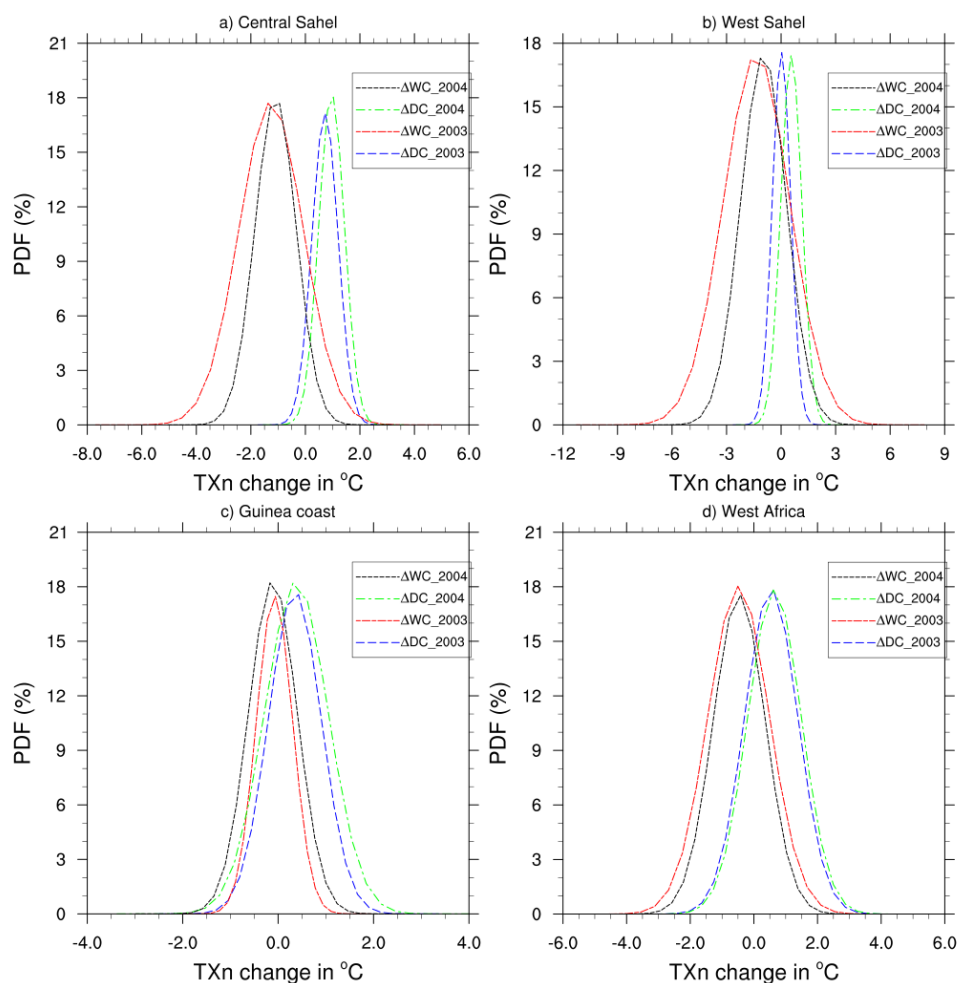
1140

1141

1142



1143  
1144  
1145

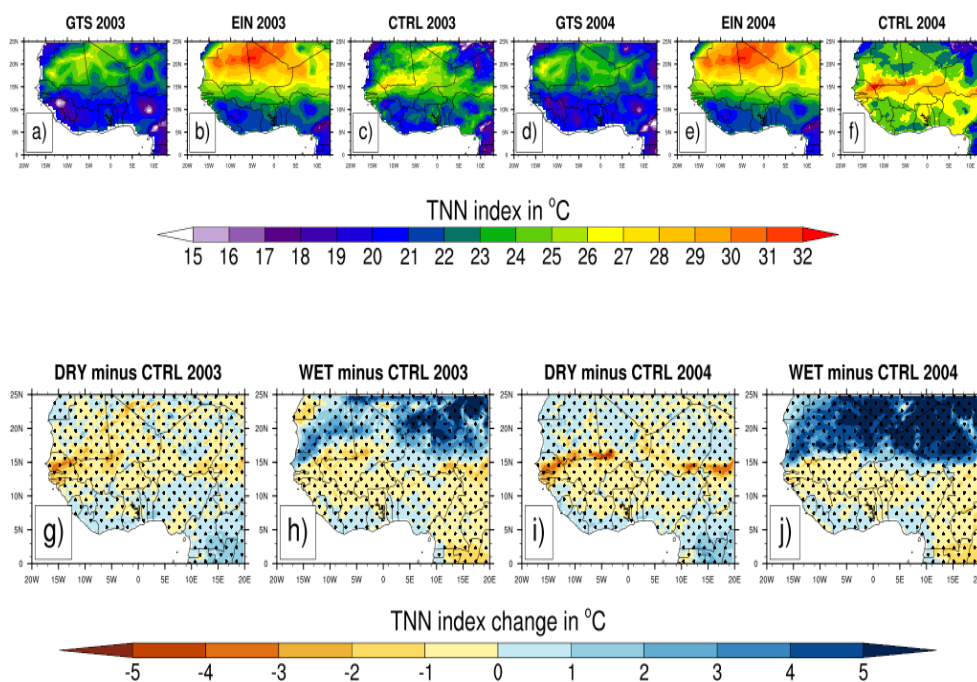


1146  
1147  
1148  
1149  
1150  
1151  
1152  
1153

**Figure 17:** Same as Fig. 15 but for the TXn index.



1154  
1155  
1156



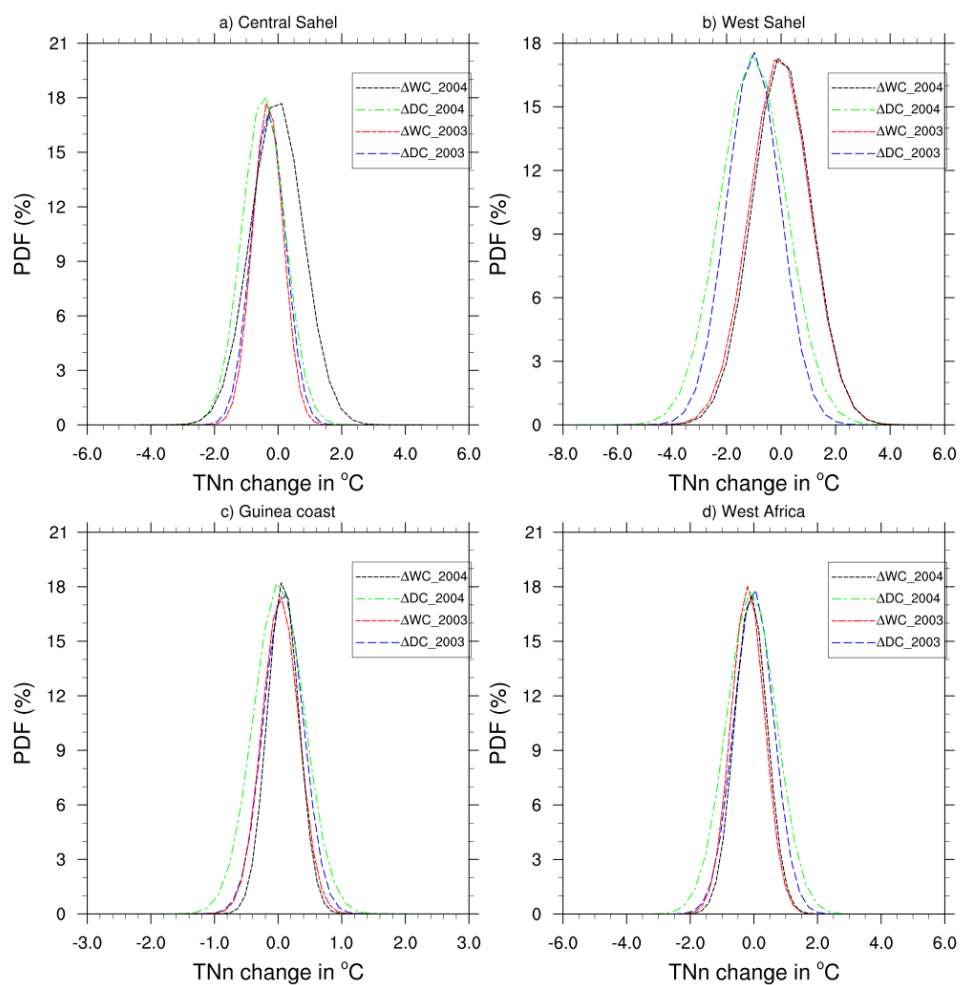
1157  
1158  
1159  
1160  
1161  
1162  
1163  
1164  
1165  
1166  
1167  
1168  
1169  
1170  
1171  
1172

**Figure 18:** Same as Fig. 14 but for the TNN index.





1173  
1174  
1175

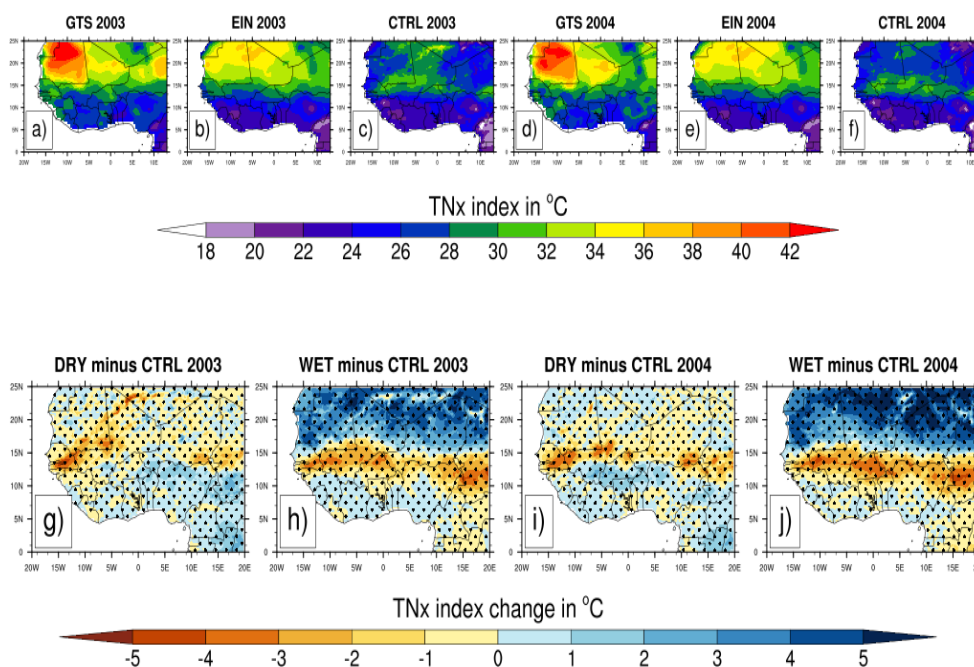


1176  
1177  
1178  
1179  
1180  
1181  
1182  
1183

**Figure 19:** Same as Fig. 14 but for the TNn index.



1184  
1185  
1186

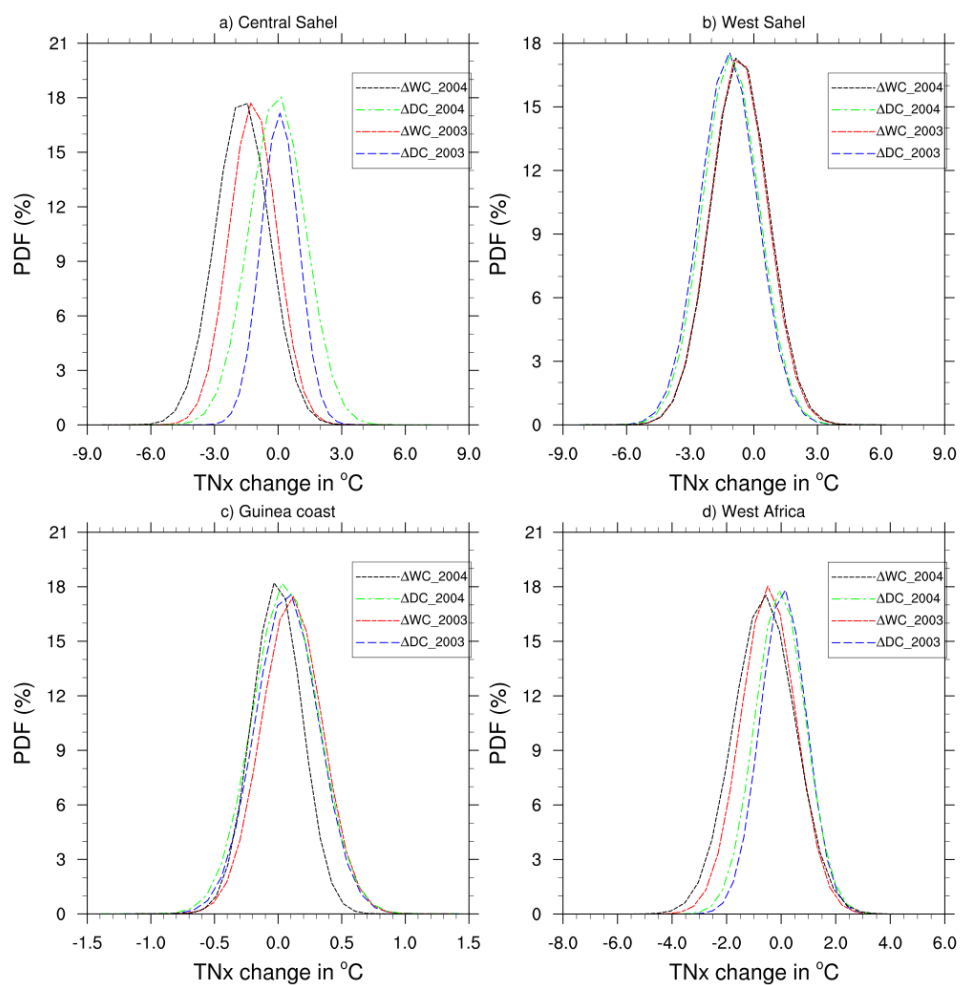


1187  
1188  
1189  
1190  
1191  
1192  
1193  
1194  
1195  
1196  
1197  
1198  
1199  
1200  
1201  
1202  
1203

**Figure 20:** Same as Fig. 14 but for the TNx index



1204  
1205  
1206



1207  
1208  
1209  
1210  
1211

**Figure 21:** Same as Fig. 15 but for the TNx index.